

REPORT DOCUMENTATION PAGE

ITIC FILE COPY

AD-A205 197 **ITIC****ECTE**

1b RESTRICTIVE MARKINGS

3 DISTRIBUTION/AVAILABILITY OF REPORT
Approved for public release;
distribution is unlimited. (2)DECLASSIFICATION/DOWNGRADING SCHEDULE
FEB 17 1989

4. PERFORMING ORGANIZATION REPORT NUMBER(S)

5. MONITORING ORGANIZATION REPORT NUMBER(S)

AFOSR-TR-89-0220

6a. NAME OF PERFORMING ORGANIZATION

Univ of Illinois

6b. OFFICE SYMBOL
(if applicable)

D CS

7a. NAME OF MONITORING ORGANIZATION

AFOSR/NP

6c. ADDRESS (City, State, and ZIP Code)

P. O. Box 6998
Chicago, IL 60680

7b. ADDRESS (City, State, and ZIP Code)

Building 410, Bolling AFB DC
20332-64488a. NAME OF FUNDING / SPONSORING
ORGANIZATION

AFOSR

8b. OFFICE SYMBOL
(if applicable)

NP

9 PROCUREMENT INSTRUMENT IDENTIFICATION NUMBER

F49620-85-K-0020

8c. ADDRESS (City, State, and ZIP Code)

Building 410, Bolling AFB DC
20332-6448

10. SOURCE OF FUNDING NUMBERS

PROGRAM
ELEMENT NO.

61102F

PROJECT
NO.

2301

TASK
NO.

A1

WORK UNIT
ACCESSION NO

11 TITLE (Include Security Classification)

(U) STUDIES OF COLLISIONAL AND NONLINEAR RADIATIVE PROCESSES FOR DEVELOPMENT OF COHERENT UV AND XUV SOURCES

12. PERSONAL AUTHOR(S)

13a. TYPE OF REPORT
FINAL13b. TIME COVERED
FROM 30 Sep 85 TO 29 Sep 88

14. DATE OF REPORT (Year, Month, Day)

15. PAGE COUNT
75

16. SUPPLEMENTARY NOTATION

17. COSATI CODES

FIELD	GROUP	SUB-GROUP
	2006	

18 SUBJECT TERMS (Continue on reverse if necessary and identify by block number)

19. ABSTRACT (Continue on reverse if necessary and identify by block number)

A laboratory means for the generation of ultrahigh energy density states of matter, corresponding approximately to 0.1 - 1.0 W/atom at solid density, is currently underdevelopment. This enables the production, in a convenient laboratory environment, of energy densities comparable to those occurring in the thermonuclear environments and stellar interiors. The method being developed in the University of Illinois laboratory involves a unique combination of three basic elements. They are (a) a new extremely high-peak-power ultraviolet laser technology (femtosecond rare gas halogen systems), (b) energy deposition stemming from high-order multiphoton processes, and (c) a mode of channeled propagation that arises in the strong-field regime. The compatibility of these three independent considerations is a key and unique feature of the approach. The use of this technology will permit the study of new realms of atomic phenomena. (jtd)

20. DISTRIBUTION/AVAILABILITY OF ABSTRACT

 UNCLASSIFIED/UNLIMITED
 SAME AS RPT
 DTIC USERS
21 ABSTRACT SECURITY CLASSIFICATION
UNCLASSIFIED

22a. NAME OF RESPONSIBLE INDIVIDUAL

H R Schlossberg

22b. TELEPHONE (Include Area Code)

202/767-4906

22c. OFFICE SYMBOL

AFOSR/NP



THE
UNIVERSITY
OF
ILLINOIS
AT
CHICAGO

Laboratory for Atomic, Molecular, and Radiation Physics (M/C 273)
Department of Physics
College of Liberal Arts and Sciences
Box 4348, Chicago, Illinois 60680
(312) 996-4868

AFOSR-TR-89-0220

17 November 1988

Final Technical Report Covering:
Contract No.: F49620-85-K-0020

30 SEP 85 - 29 SEP 88

**STUDIES OF COLLISIONAL AND NONLINEAR RADIATIVE
PROCESSES FOR DEVELOPMENT OF COHERENT UV AND XUV SOURCES**

Principal Investigator: Charles K. Rhodes

Co-Investigators: Keith Boyer
Ting S. Luk

Prepared for: Dr. Howard Schlossberg
AFOSR/NP
Building 410, Room C219
Bolling Air Force Base
Washington, D. C. 20332

89 2 15 107

Table of Contents

Record of Publications Conducted with AFOSR Support (February 1988 – November 1988)	i
ABSTRACT	iii
I. INTRODUCTION	1
II. DISCUSSION OF RESEARCH AREAS	3
A. Ultrahigh Brightness Subpicosecond Laser Technology	3
B. Behavior of Atomic and Molecular Matter in Very Strong Fields	7
C. Highly Stripped Ions	9
D. Dense Non-Equilibrium Plasmas	12
E. Modes of Electromagnetic Propagation in the Strong-Field Regime	12
F. Optically Induced Nuclear Processes	14
III. CONTROLLED ENERGY DEPOSITION – SUMMARY	14
IV. CONCLUSIONS	16
V. REFERENCES	17
VI. APPENDICES	21
Appendix A: "Kinetic Energy Distributions of Ionic Fragments Produced by Subpicosecond Multiphoton Ionization of N ₂ "	21
Appendix B: "Possibility of Optically Induced Nuclear Fission"	46
Appendix C: "Measurement of 248-nm, Subpicosecond Pulse Durations by Two-Photon Fluorescence of Xenon Excimers"	51
Appendix D: "Measurement of 248-nm Focal Volume Spatial Profiles"	55
Appendix E: "Characteristics of a Non-Equilibrium Picosecond Laser Plasma"	59
Appendix F: "X-Ray Amplification with Charge-Displacement Self-Channeling"	65

Accession For	
NTIS CRA&I	<input checked="" type="checkbox"/>
DTIC TAB	<input type="checkbox"/>
Unannounced	<input type="checkbox"/>
Justification	
By	
Distribution /	
Availability Codes	
Dist	Avail and/or Special
A-1	

Record of Publications Conducted with AFOSR Support (February 1988 - November 1988):

1. "Possibility of Optically Induced Nuclear Fission," K. Boyer, T. S. Luk, and C. K. Rhodes, *Phys. Rev. Lett.* **60**, 557 (1988).
2. "Discussion of the Role of Many-Electron Motions in Multiphoton Ionization and Excitation," K. Boyer, H. Jara, T. S. Luk, I. A. McIntyre, A. McPherson, R. Rosman, J. C. Solem, C. K. Rhodes, and A. Szöke, Proceedings of ICOMP IV, ed. S. J. Smith and P. L. Knight (Cambridge University Press, Cambridge, 1987) p. 58.
3. "Discussion of Limiting Deposition Power Densities in Laser Target Materials," A. McPherson, K. Boyer, H. Jara, T. S. Luk, I. A. McIntyre, R. Rosman, J. C. Solem, and C. K. Rhodes, Atomic and Molecular Processes with Short Intense Laser Pulses, ed. André D. Bandrauk (Plenum Press, NY, 1988) p. 165.
4. "Generation of IR and XUV Radiation in Krypton with Picosecond Irradiation at 193 nm," M. Shahidi, T. S. Luk and C. K. Rhodes, to be published in *JOSA B*.
5. "Fifth-Harmonic Production in Neon and Argon with Picosecond 248-nm Radiation," R. Rosman, G. Gibson, K. Boyer, H. Jara, T. S. Luk, I. A. McIntyre, A. McPherson, J. C. Solem, and C. K. Rhodes, *J. Opt. Soc. Am. B* **5**, 1237 (1988).
6. "Tunable Hybrid Mode-Locked Dye Laser Operating in the Range 735 - 760 nm," I. A. McIntyre, K. Boyer, and C. K. Rhodes, *Optics Communications* **67**, 225 (1988).
7. "Corresponding Aspects of Strong-Field Multiquantum Processes and Ion-Atom Collisions," K. Boyer, G. Gibson, H. Jara, T. S. Luk, I. A. McIntyre, A. McPherson, R. Rosman, J. C. Solem, and C. K. Rhodes, *IEEE Transactions on Plasma Science*, in press.
8. "The Influence of Free Electrons on the Propagation of Intense Subpicosecond 248 nm Radiation in Hydrogen Plasmas," T. S. Luk, X. J. Pan, J. C. Solem, K. Boyer, and C. K. Rhodes, in the proceedings of the O-E/LASE '88 Conference, 10 - 15 January 1988, Los Angeles, CA, to be published by SPIE.
9. "High Power Excimer Lasers," I. A. McIntyre and C. K. Rhodes, submitted to *Applied Physics Review*.
10. "XUV Spectroscopy of Ions Produced by Multiphoton Absorption," K. Boyer, G. Gibson, H. Jara, T. S. Luk, I. A. McIntyre, A. McPherson, R. Rosman, J. C. Solem, and C. K. Rhodes, to be published in *The Proceedings of RIS '88*, 10 - 15 April 1988, NBS, a volume in *The Institute of Physics Conference Series*, by IOP Publishing Ltd.
11. "Multiphoton Dissociative Ionization of Molecular Deuterium," T. S. Luk and C. K. Rhodes, *Physical Review A*, in press.

12. "Kinetic Energy Distributions of Ionic Fragments Produced by Subpicosecond Multiphoton Ionization of N_2 ," K. Boyer, T. S. Luk, J. C. Solem, and C. K. Rhodes, *Physical Review A*, in press.
13. "Research on Strong Field Processes with a Subpicosecond 400 GW Ultraviolet Source," T. S. Luk, K. Boyer, G. Gibson, H. Jara, I. A. McIntyre, A. McPherson, X. J. Pan, R. Rosman, X. M. Shi, C. K. Rhodes, and J. C. Solem, presented at the LM & LS '88 Conference, 25 - 27 July 1988, Shanghai, China, to be published.
14. "Charge-Displacement Self-Channelling as a Method for Energy Concentration," K. Boyer, T. S. Luk, J. C. Solem and C. K. Rhodes, to be published in the OSA Proceedings on Short Wavelength Coherent Radiation: Generation and Application, 26 - 29 September 1988, Cape Cod, Massachusetts, edited by R. W. Falcone and J. Kirz.
15. "Strong-Field Processes in the Ultraviolet Region," K. Boyer, G. Gibson, H. Jara, T. S. Luk, I. A. McIntyre, A. McPherson, R. Rosman, C. K. Rhodes, and J. C. Solem, to be published in the OSA Proceedings on Short Wavelength Coherent Radiation: Generation and Application, 26 - 29 September 1988, Cape Cod, Massachusetts, edited by R. W. Falcone and J. Kirz.
16. "Characteristics of a Non-Equilibrium Picosecond Laser Plasma," G. Gibson, R. Rosman, T. S. Luk, I. A. McIntyre, A. McPherson, G. Wendin, K. Boyer and C. K. Rhodes, to be published in the OSA Proceedings on Short Wavelength Coherent Radiation: Generation and Application, 26 - 29 September 1988, Cape Cod, Massachusetts, edited by R. W. Falcone and J. Kirz.
17. "X-Ray Amplification with Charge-Displacement Self-Channelling," J. C. Solem, T. S. Luk, K. Boyer and C. K. Rhodes, submitted to *Phys. Rev. Lett.*, 29 September 1988.
18. "Research on Strong-Field Processes in the Ultraviolet Region," K. Boyer, G. Gibson, H. Jara, T. S. Luk, I. A. McIntyre, A. McPherson, R. Rosman, C. K. Rhodes, and J. C. Solem, presented at the NATO Advanced Study Institute, Atoms in Strong Fields, Kos, Greece, October 1988, to be published.

ABSTRACT

A laboratory means for the generation of ultrahigh energy density states of matter, corresponding approximately to $0.1 - 1.0$ W/atom at solid density, is currently under development. This enables the production, in a convenient laboratory environment, of energy densities comparable to those occurring in thermonuclear environments and stellar interiors. The method being developed in our laboratory involves a unique combination of three basic elements. They are (a) a new extremely high-peak-power ultraviolet laser technology (femtosecond rare gas halogen systems), (b) energy deposition stemming from high-order multiphoton processes, and (c) a mode of channeled propagation that arises in the strong-field regime. The compatibility of these three independent considerations is a key and unique feature of the approach. The use of this technology will permit the study of new realms of atomic phenomena. Specifically, the areas involve (1) ultrahigh brightness laser technology, (2) the behavior of matter in very strong fields, (3) the properties of highly stripped ions, (4) the characteristics of dense highly non-equilibrium plasmas, (5) new high-field modes of electromagnetic propagation, and (6) the possibility of a laser-driven means for the excitation and control of nuclear reactions.

I. INTRODUCTION

The availability of an ultraviolet laser technology^{1,2} capable of producing subpicosecond pulses with energies at the joule level in low divergence beams at high repetition rates is making possible a new regime of laboratory scale physical study concerning the behavior of matter at extremely high energy densities and field strengths.^{3,4} With this new experimental means, a maximum electric field strength E on the order of $100 (e/a_0^2)$ should be attainable, a condition that will permit the generation of energy densities associated with coherently driven motions comparable to or possibly exceeding those characteristic of thermonuclear conditions. Moreover, an electric amplitude of this magnitude at ultraviolet wavelengths will cause the development of strongly relativistic⁵⁻⁸ electronic motions with an energy scale comparable to typical nuclear binding energies. This is a new and totally unexplored regime of physical conditions.

Several important implications stem directly from the technical capability to generate such unusually high energy densities and strong electromagnetic forces. Foremost, it is expected that atomic and molecular material will respond in very unusual ways to such severely perturbed conditions and it has been conjectured, in contrast to interactions associated with weak fields, that fundamentally different types of electronic motions⁹ may be driven under such extreme conditions of irradiation. At the outset, therefore, we expect, in comparison to the normal weakly excited conditions, significant modifications of (1) the properties of electromagnetic interaction with free atoms, (2) the behavior of dense plasmas, and (3) the modes of electromagnetic propagation occurring through such highly excited material.

Considerable data support the conclusion that very high deposition rates can be achieved in materials as a consequence of the strong electromagnetic perturbations.

This view is based on the accumulating evidence, derived from both experimental findings^{4,10} and theoretical analyses,¹¹ that extremely high peak energy transfer rates can be achieved. For example, recent studies¹² of the kinetic energy distributions of ionic fragments produced by multiphoton ionization of N₂, as outlined in Appendix A, and other molecules¹³ clearly indicate that the major fraction of the energy transfer occurs over a maximum time interval bounded by a few cycles of the wave. For the case of N₂ at an intensity of $\sim 10^{16}$ W/cm² with 248-nm radiation, a peak rate on the order of a few milliwatts/molecule was inferred from this work. It is projected¹¹ that for higher intensities, in the range of $10^{19} - 10^{20}$ W/cm², the rate may approach a value of ~ 1 W/atom, particularly for heavy materials. The implication is a transferred energy in the range of ~ 100 keV/atom, a magnitude sufficient to lead to ionization of electrons in the L-shell of uranium (~ 21 keV).

It is important to realize that this estimate is not an enormous extrapolation from existing experimental results. As described below, radiation from Ar⁹⁺ has been observed from a state (2s2p⁸), a level that lies more than 1.1 keV above that of the neutral atom ground state. Ionization¹⁴ of the L-shell of Ar⁹⁺ alone requires 0.42 keV.

Overall, the evidence points overwhelmingly to the conclusion that states of matter involving very high energy densities, on the order of ~ 1 W/atom at solid density ($\sim 10^{22}$ W/cm³), can be studied at a high data rate by relatively simple laboratory means. Furthermore, since the time scale for the production of these conditions is extremely short (~ 100 fs), unusual plasmas far from equilibrium conditions will clearly be generated. The study of such physical conditions will certainly lead to many new insights on the non-equilibrium properties of extremely high energy density states of matter. Furthermore, since the basic task in the

production of coherent short wavelength radiation is the controlled deposition of energy at high specific powers, we can anticipate the development of bright laboratory scale x-ray sources as a natural derivative of this capability. This, of course, is a central goal of our work.

In summary, our research program involves (1) the further development of an ultrahigh brightness ultraviolet laser technology to serve the study of (2) the fundamental behavior of atomic material in very strong fields ($E \gg e/a_0^2$), (3) the properties of highly stripped ions, (4) the characteristics of dense non-equilibrium plasmas, and (5) the modes of electromagnetic propagation occurring under extreme conditions of material excitation. These five topics all represent frontiers in the realm of atomic phenomena and are areas of strong relevance to advanced defense concepts. Finally, there is a sixth subject, although not strictly limited to the atomic domain, in which important fundamental information should be produced in the proposed program. It involves the coupling of atomic and nuclear degrees of freedom with the possible outcome that a new means for the control of nuclear reactions would become available. A range of possibilities exists for various nuclear systems,¹⁵⁻¹⁸ including that of fission,¹⁹ as outlined in Appendix B.

II. DISCUSSION OF RESEARCH AREAS

A. Ultrahigh Brightness Subpicosecond Laser Technology

Since the feasibility of the new physical research being conducted is fundamentally predicated on the availability of bright high-peak-power ultraviolet sources, we describe the development of those sources and the performance limits that can be achieved.

The present operating KrF* (248 nm) system, which incorporates a large aperture (100 cm²) power amplifier, is illustrated in Fig. (1). The pulse duration measurement system²⁰ and pulse spatial measurement apparatus are described in Appendix C

SUBPICOSECOND KrF⁺ LASER SYSTEM at the University of Illinois at Chicago

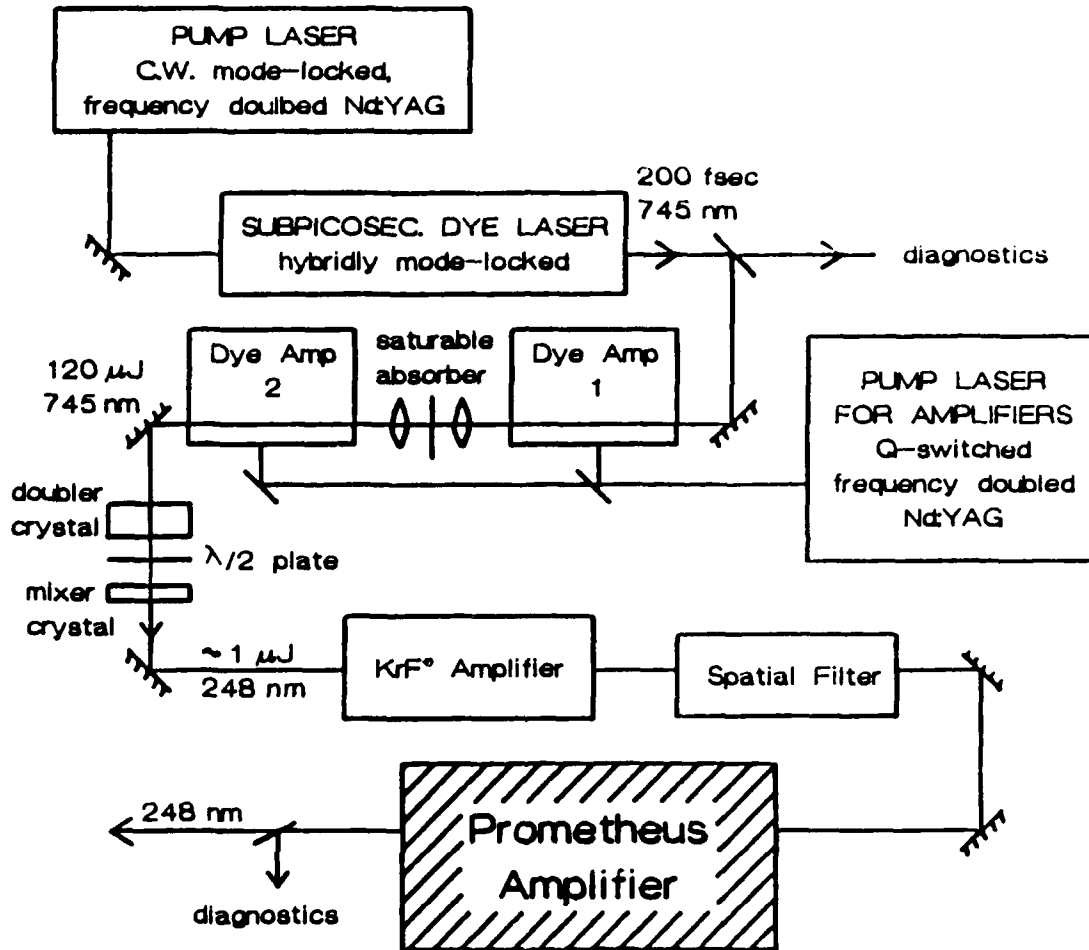


Fig. (1): Schematic of high brightness subpicosecond source incorporating a large aperture (100 cm²) power amplifier (Prometheus).

and Appendix D, respectively. The development of the diagnostics described in these appendices gives confidence that we are obtaining a good experimental understanding of the operation of these light sources and can, therefore, reliably access the performance limits of the technology.

Three steps are currently being taken to increase the available intensity. They are (1) the use of a fast $f/2$ optical system, (2) the use of shorter pulses^{21,22} (~ 100 fs) in the amplifier chain, and (3) the optimization of the large aperture (100 cm^2) power amplifier delivered in February 1988 to further increase the pulse energy.

We now discuss the measured parameters of the currently operating system and compare them to the limiting values that we feel the system can attain with suitable optimization. Presently, the output energy is measured as ~ 350 mJ in a pulse length of ~ 600 fs. These are the parameters delivered at the end of the beam line at the experimental stations. The pulse width of ~ 365 fs described in Appendix C has been broadened to some extent by the effect of group velocity dispersion arising from the additional optical elements associated with the large aperture power amplifier. This pulse broadening effect can be eliminated by known techniques²³ of compensation using either prisms or gratings. In addition, shorter pulses can be generated with a modified source for the production of the seed beam.

An essential parameter governing the brightness of the 248-nm source is the focal spot size that can be achieved. Therefore, the ability to produce a small focal volume was one of the chief design criteria for the large aperture system. The result of a measurement on the beam profile at a point after the power amplifier, using the configuration shown in Appendix D, is illustrated in Fig. (2). A focal diameter of $\sim 1.4 \mu\text{m}$, produced with an $f/2$ optical system, is shown, a

FOCAL SPOT SIZE (248 nm)

(after power amplifier)

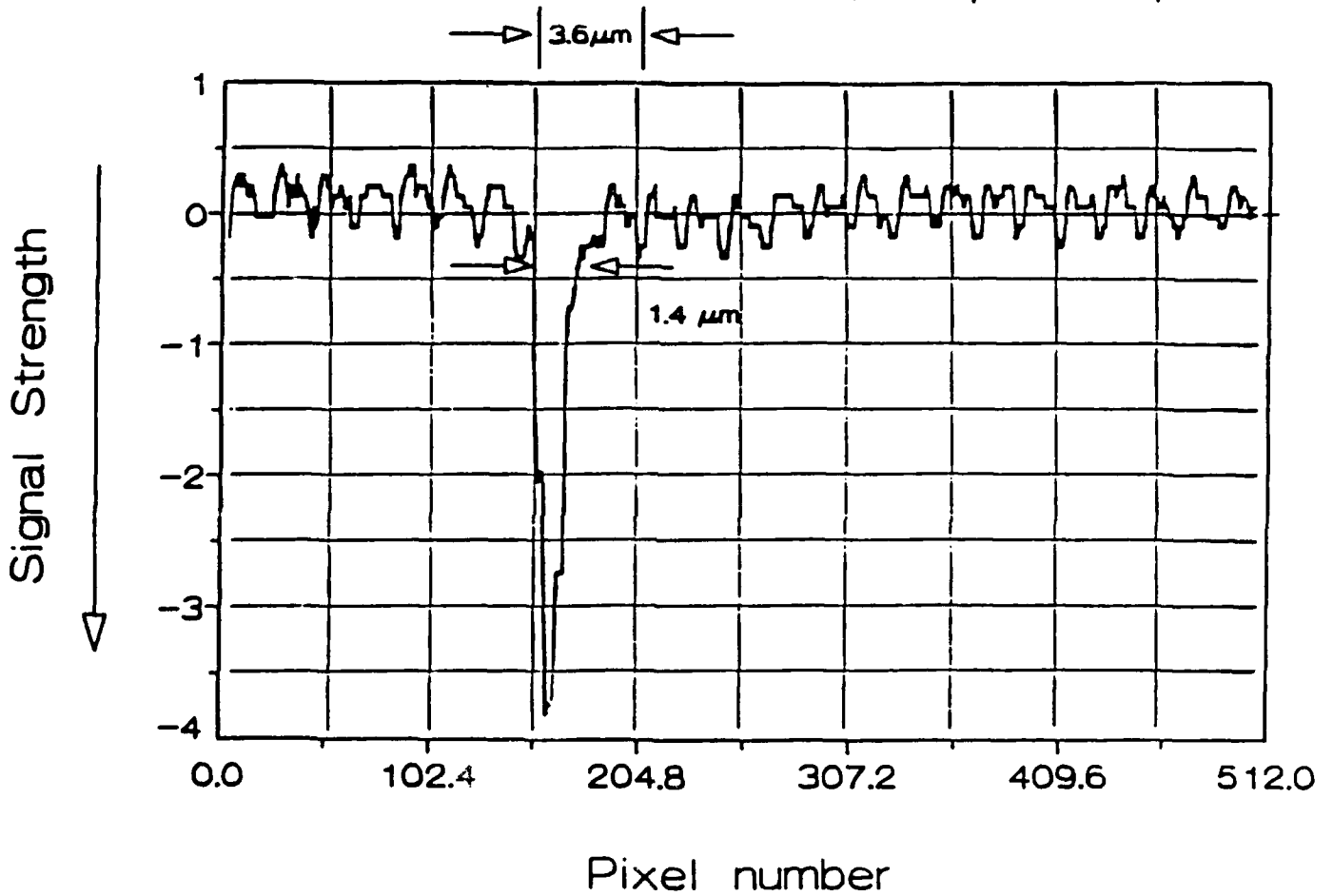


Fig. (2): Spatial profile of focal spot recorded after the power amplifier with configuration described in Appendix D. A spot diameter of $\sim 1.4 \mu\text{m}$ is measured.

value very close to the diffraction limit ($\sim 0.9 \mu\text{m}$). Further refinement of the system may enable this diameter to be reduced to the $\sim 1.0 - 1.2 \mu\text{m}$ range.

The present capability of the source, based on the measurements described above, is summarized in Table I. A maximum intensity $I \approx 3.8 \times 10^{19} \text{ W/cm}^2$ is derived, a value only slightly below the Compton intensity,^{5,7} $I_{\text{CO}} \approx 4.5 \times 10^{19} \text{ W/cm}^2$.

These current parameters of performance can be compared with the values believed to be reasonable achievable figures for the system being developed. The comparisons are presented in Table II. In terms of the maximum electric field, or equivalently, the force that can be exerted on a charged particle, the present system is within a factor of six of the limiting value believed to apply for this instrument.

B. Behavior of Atomic and Molecular Matter in Very Strong Fields

A research effort is currently underway in this Laboratory whose goal is the understanding of the nonlinear processes governing the coupling of intense radiation to atomic and molecular matter. The general amplitude under study is



a process which, overall, produces ions, electrons and photons.

Although certainly far from complete, this work has revealed several important characteristics of the strong field interaction.

In the effort to understand the coupling represented by process (1), the properties of ion charge state distributions,²⁴ electron energy spectra,^{25,26} and both fluorescence and harmonic radiation^{4,10} produced by irradiation of atoms with intense ultraviolet radiation have been investigated. The substantial body of information contained in earlier work concerning the ion and electron distributions is documented extensively in references^{3,4,24,25,26} and associated citations.

Theoretically, the picture is diverse and controversial. The models describing

Table I: Summary of Current Operating Parameters of 248-nm System

Brightness and Intensity

$$I = \frac{E}{\tau A} = \frac{4E}{\tau \pi d^2} \text{ W/cm}^2$$

Measured Quantities:

- $E \approx 350 \text{ mJ}$ (output energy)
- $\tau \approx 600 \text{ fs}$ (after power amplifier)
- $d = 1.4 \text{ }\mu\text{m}$ (after power amplifier)

Derived Quantities:

- $I \approx 3.8 \times 10^{19} \text{ W/cm}^2$
- $\frac{E}{A} \approx 2.3 \times 10^7 \text{ J/cm}^2$

Table II: Comparison of Current and Projected Operating Parameters for the 248-nm System

Parameter	Current Measured Value	Projected Developed Value
Pulse Energy (J)	~ 0.350	1.0
Pulse Width (fs)	~ 600	100
Focal Spot Diameter (μm)	~ 1.4	1.0 - 1.2
Maximum Intensity (W/cm^2)	3.8×10^{19}	~ 10^{21}
Maximum Electric Field (V/cm)	~ 1.5×10^{11}	~ 9×10^{11}
Pulse Repetition Rate (s^{-1})	0.5	1.0

the electronic motion under strong fields range from those involving sequential electron emission²⁷ on one hand to others which consider the consequences of more organized multi-electron motions.^{9,28,29} The role of screening has been evaluated³⁰ and analogies with atomic,²⁸ ionic,³¹ and electronic³² collisions have been discussed.

At the present, for the most interesting regime in which the external field is far larger than an atomic unit, no comprehensive theory exists and the experimental capability is just now, as discussed in Section II.A above, permitting study of that important region. Naturally, we intend to concentrate our future experimental activity in this area. Experimentally, we have found that two basic types of study, (1) collision-free ion experiments and (2) the spectroscopy of emitted radiation, effectively complement one another in terms of the physical information derived. Moreover, the former is performed at very low density in order to eliminate collisions, while the latter is commonly conducted in a region of target density in which collisional processes may become significant.

C. Highly Stripped Ions

Comparison of the observed levels of ionization with the Keldysh³³ curve indicates a systematic behavior which assists in the construction of an approximate extrapolation to the very high-field regime ($E \gg e/a_0^2$). So far, the extant data give the following indications.⁴

The ion time-of-flight technique has been used to measure the threshold laser intensities for all charge states of the rare gases which appear below 10^{16} W/cm² with subpicosecond irradiation at 248 nm. The experimental values are plotted in Fig. (3) as functions of the ionization energies for each charge state. They are compared to calculated threshold laser intensities for a transition probability of about 10^{-9} , the value which corresponds to the estimated detection limit of the

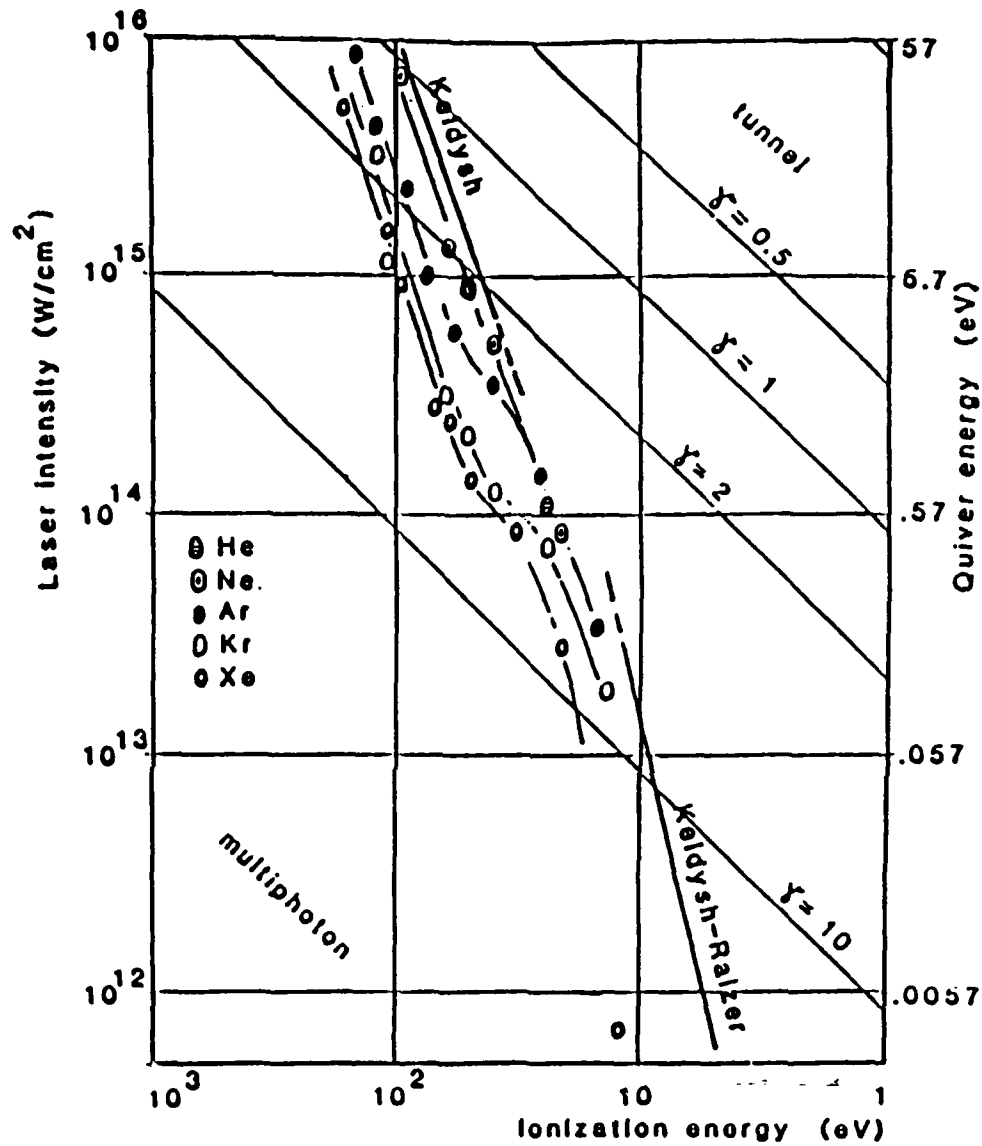


Fig. (3): Threshold laser intensity for ion charge state production with a 248-nm \sim 500-fs laser pulse. A transition probability of $T \approx 10^{-3}$ has been assumed for the calculation (estimated detection limit). The quiver energy corresponding to a free electron in the radiation field is also shown on the right-hand ordinate.

apparatus, using Keldysh's result³³ (including coulomb correction) in the tunneling approximation ($\gamma \ll 1$) and the Keldysh-Raizer formula³⁴ in the multiphoton approximation ($\gamma \gg 1$). The observed thresholds for neon, which range from $\sim 8 \times 10^{13}$ W/cm² (Ne⁺) to $\sim 7 \times 10^{15}$ W/cm² (Ne¹⁰⁺), agree remarkably well with the calculations, whereas the corresponding thresholds are consistently below the Keldysh curve for the heavier ions. For heavy systems, the deviation is considerable, the point for xenon at an ionization energy of ~ 100 eV being approximately a full order of magnitude below the Keldysh line.

Extrapolation³⁵ of the Keldysh result, taking into account the deviation shown in Fig. (3), leads to the following approximate predictions for ion production under collision-free conditions. At an intensity of $\sim 10^{19}$ W/cm², uranium would exhibit ionization of electrons in the 4p-shell with the production of species in the vicinity of U⁶⁰⁺. For a greater intensity of $\sim 10^{21}$ W/cm², gold would be ionized down to approximately Au⁶⁹⁺, the neon-like state. A further increase in intensity of roughly a factor of four would produce uranium in charge states near U⁸²⁺. Although these estimates must be regarded as extremely rough, all the available evidence points to the production of very high charge states under the intense field conditions that can be produced by the laser technology described in Section II.A above. Finally, we point out that, although highly charged ions can be produced in detectable quantities by other means, such as EBIS³⁶ and EBIT³⁷ systems, the ion densities and ion formation rates characteristic of the laser approach are many orders of magnitude greater.

The ability to rapidly produce highly ionized species over a large range of medium density will unquestionably enable the study of many of their structural properties and interactions. This would naturally include relativistic effects in the ionic structure,³⁸ affecting both the systematics of the energy levels and the

transition probabilities,³⁹ in addition to a range of collisional processes⁴⁰ such as those involved in recombination.⁴¹ It is important to observe that the short time scale of production characteristic of the laser method (≈ 1 ps) would permit time resolution of the recombination process, thereby experimentally rendering a detailed picture of the dynamics not readily obtained by steady-state means.

D. Dense Non-Equilibrium Plasmas

An obvious implication of the discussion in Section II.C is the ability to generate dense non-equilibrium plasmas at energy and power densities comparable to thermonuclear conditions. The preliminary experiments described in Appendix E give a feeling for the nature of the physical conditions that can be produced and data that can be readily obtained. Naturally, the streak camera system we are now constructing will substantially enhance that capability.

The unusual plasma states that can be generated have several salient features. In the main, they have a high level of ionization, relatively low electron heating, negligible ion heating, and utterly insignificant heavy body hydrodynamic motion. Such circumstances are expected to result in a range of anomalous characteristics, such as enhanced rates of recombination and other properties associated with the line profiles^{42,43} of radiators embedded in the plasma environment.

E. Modes of Electromagnetic Propagation in the Strong-Field Regime

It appears⁴⁴⁻⁴⁶ that a fundamentally new regime of electromagnetic propagation may develop in plasmas for subpicosecond radiation of sufficient intensity. In the high intensity case of interest, in which processes generating ionization dominate the coupling, multiphoton ionization is expected to produce a substantial reduction of both the linear and nonlinear refractive indices of the medium. For a suitably ionized plasma, this combination of high charge state ions with the electron density produced by the multiphoton coupling appears capable of producing a new

mode of radiative channeling. Indeed, preliminary analysis,⁴⁷ as described in Appendix F, supports the presence of the following mechanism. For a sufficiently short pulse (~ 100 fs), the massive ions remain spatially fixed while the relatively mobile electrons are expelled by the ponderomotive force from the high intensity zone. Thereby, a state of equilibrium is established between the ponderomotive and the electrostatic force densities owing to the charge displacement. Since the electrons, which embody a negative contribution to the index, are expelled, an on-axis region of relatively high refractive index is formed which supports the channeling. In a limiting case, it appears that the behavior approaches that characteristic of a metallic waveguide. Interestingly, a focusing mechanism of this type, which is governed principally by the intensity, is not describable in terms of the conventional nonlinear index parameter n_2 and the customary concept of a critical power does not apply.⁴⁸ A further unusual aspect of this process, since there is a strong tendency to locally reduce the plasma frequency ω_p in the region where the intensity is high, is that it may enable propagation for appreciable distances in plasmas that would normally be considered as overdense. If so, we would then have the optical analogue of the armor piercing shell.

A striking aspect of the analysis presented in Appendix F is the extremely strong frequency dependence favoring the use of ultraviolet wavelengths to establish the conditions for channeling. Scaling laws⁴⁷ indicating variations as rapid as ω^9 are derived.

The critical intensity I_c for 248-nm radiation theoretically estimated in Appendix F for the onset of this phenomenon is $I_c \approx 2.4 \times 10^{19}$ W/cm², a value below that shown in Table II as the present capability. Therefore, we are now in a position to explore the regime of intensity both in the vicinity of I_c and somewhat above it.

F. Optically Induced Nuclear Processes

A basic question concerns the ability to couple laser excited electronic motions to nuclear degrees of freedom.¹⁵⁻¹⁹ Direct coupling to the nucleus is expected to be negligible, since nuclear matrix elements are extremely small and since the tightly bound innermost electrons in heavy atoms tend to shield the nucleus from the optical field.⁴⁹ It appears, however, that, in the strongly relativistic regime, the coupling of the driven electronic motions is sufficient to induce nuclear processes. An example is electrofission, as discussed in Appendix B, a reaction for which estimates¹⁹ indicate clearly observable yields under conditions that can be produced with the large aperture system. The detection of fission fragments, which can be experimentally accomplished with very high sensitivity, would constitute an utterly undeniable signature of this process. Furthermore, since there is independent knowledge of relevant nuclear properties and cross sections, the electronically induced nuclear processes can serve as a probe of the energetic electronic motions driven by the intense irradiation. This aspect presents the possibility that these types of processes can be used to determine the nature of the electronic motions occurring in the high field regime at an intensity level of $\sim 10^{21}$ W/cm².

III. CONTROLLED ENERGY DEPOSITION - SUMMARY

The research described in this document addresses the basic question of the controlled deposition of energy at high specific powers. The answer that emerges involves three separate considerations. They are (1) a new ultraviolet pulsed power technology, (2) an energy deposition mechanism based on highly nonlinear coupling, and (3) a condition for channeled propagation. It can be seen that these three elements, which appear capable of producing conditions comparable to, or possibly exceeding those of a thermonuclear environment, fit together in a remarkably congenial way. Figure (4) illustrates these relationships. The principal issue is

Multiphoton Energy Transfer Cross Section

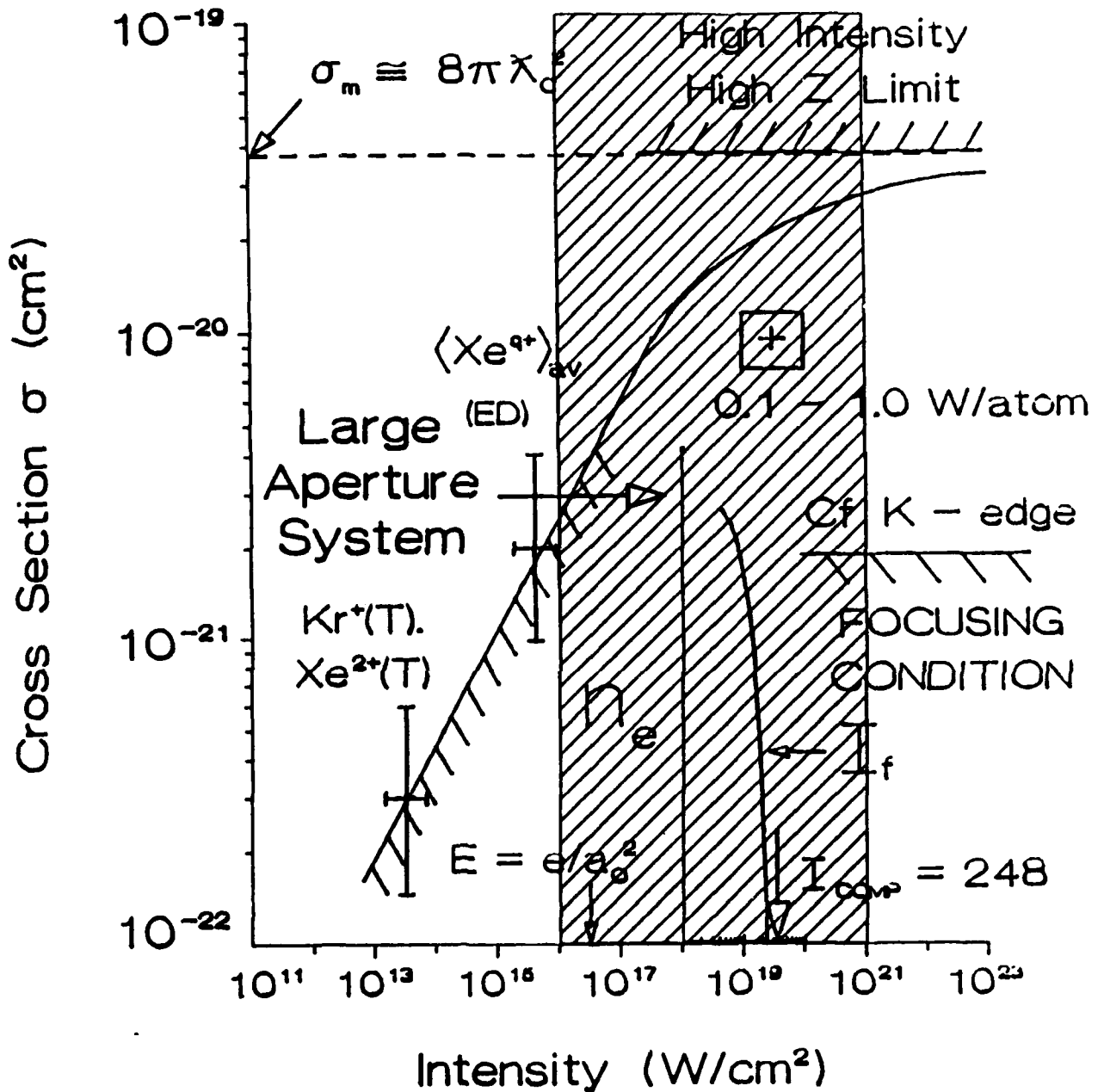


Fig. (4): Illustration of how (1) the energy transfer cross section, (2) the channeling condition, and (3) the pulse power technology all fit together. The significant fact is that the conditions needed for the strong multiphoton coupling governing the energy transfer ($I \approx I_{co} \approx 10^{19} W/cm^2$) are identical to those required for the channeled propagation ($I_f \approx I_{co} \approx 10^{19} W/cm^2$) and that the large aperture system moves us into the desired range. The compatibility of these three independent considerations is a key and unique feature of the approach.

that the radiative conditions needed for the strong multiphoton coupling governing the energy transfer rate¹¹ are essentially identical to those required for the channeled propagation⁴⁷ and that the laser technology can readily produce the regime of irradiation necessary. The compatibility of these three factors is a key feature of the proposed approach for the attainment of very high energy density states of matter with laboratory scale apparatus. Extremely strong frequency scaling relations,⁴⁷ ranging as high as ω^9 , particularly favor the use of ultraviolet energy for the efficient achievement of these conditions.

IV. CONCLUSIONS

A high-data-rate laboratory-scale capability for the exploration of matter at energy densities comparable to those characteristic of a thermonuclear environments or stellar interiors would greatly enhance the ability to understand the complex behavior associated with those extreme conditions. Such experimental methods are now being developed. The use of this technology will permit the study of new realms of atomic phenomena. Specifically, the areas involve (1) ultrahigh brightness laser technology, (2) the behavior of matter in very strong fields, (3) the properties of highly stripped ions, (4) the characteristics of dense highly non-equilibrium plasmas, (5) high-field modes of electromagnetic propagation, and (6) the possibility of a laser-driven means for the excitation and control of nuclear reactions.

V. REFERENCES

1. J. H. Glowia, G. Arjavalingham, P. P. Sorokin, and J. E. Rothenberg, "Amplification of 350 fsec Pulses in XeCl Excimer Gain Modules," *Opt. Lett.* **11**, 79 (1986).
2. A. P. Schwarzenbach, T. S. Luk, I. A. McIntyre, U. Johann, A. McPherson, K. Boyer, and C. K. Rhodes, "Subpicosecond KrF*-Excimer-Laser Source," *Opt. Lett.* **11**, 499 (1986).
3. C. K. Rhodes, "Multiphoton Ionization of Atoms," *Science* **229**, 1345 (1985).
4. C. K. Rhodes, "Ordered Many-Electron Motions in Atoms and X-Ray Lasers," in Giant Resonances in Atoms, Molecules, and Solids, ed. J.-P. Connerade, J. M. Esteve, and R. C. Karnatak (Plenum Press, New York, 1987) p. 533.
5. M. J. Feldman and R. Y. Chiao, "Single-Cycle Electron Acceleration in Focused Laser Fields," *Phys. Rev.* **A4**, 352 (1971).
6. E. S. Sarachik and G. T. Schappert, "Classical Theory of Scattering of Intense Laser Radiation by Free-Electrons," *Phys. Rev.* **D1**, 2738 (1970).
7. F. V. Bunkin et A. M. Prokhorov, "Interaction des Electrons avec un Champ Intense de Rayonnement Optique," in Polarisation, Matière et Rayonnement, édité par La Societe Française de Physique (Presses Universitaires de France, Paris, 1969) p. 157.
8. I. A. McIntyre and C. K. Rhodes, "High Power Excimer Lasers," submitted to *Appl. Phys. Rev.*
9. M. Pont, N. R. Walet, M. Gavrila, and C. W. McCurdy, "Dichotomy of the Hydrogen Atom in Superintense, High-Frequency Laser Fields," *Phys. Rev. Lett.* **61**, 939 (1988).
10. C. K. Rhodes, "Physical Processes at High Field Strengths," *Physica Scripta*, **T17**, 193 (1987).
11. K. Boyer, H. Jara, T. S. Luk, I. A. McIntyre, A. McPherson, R. Rosman, and C. K. Rhodes, "Limiting Cross Sections for Multiphoton Coupling," *Revue Phys. Appl.* **22**, 1793 (1987).
12. K. Boyer, T. S. Luk, J. C. Solem, and C. K. Rhodes, "Kinetic Energy Distributions of Ionic Fragments Produced by Subpicosecond Multiphoton Ionization of N₂," *Phys. Rev. A.*, to be published.
13. L. J. Fransinski, Conference on Atoms in Strong Fields, Grainau, West Germany, 5-9 September 1988, private communication.
14. R. L. Kelly and L. J. Palumbo, "Atomic and Ionic Emission Lines Below 2000 Angstroms," NRL Report 7599 (USGPO, Washington, D.C., 1983).
15. L. C. Biedenharn, G. C. Baldwin, K. Boyer, and J. C. Solem, "Nuclear Excitation by Laser Driven Coherent Outer Shell Electron Oscillations", in AIP Conference

Proceedings No. 146, Advances in Laser Science - I, edited by W. C. Stwalley and M. Lapp (AIP, New York, 1986) p. 52.

16. L. C. Biedenharn, K. Boyer, and J. C. Solem, "Possibility of Grating by Laser-Driven Nuclear Excitation", in AIP Conference Proceedings No. 146, Advances in Laser Science - I, edited by W. C. Stwalley and M. Lapp (AIP, New York, 1986) p. 50.
17. G. A. Rinker, J. C. Solem, and L. C. Biedenharn, "Nuclear Interlevel Transfer Driven by Collective Outer Shell Electron Oscillations", LA-UR-86-4187, Los Alamos National Laboratory Report, October, 1987.
18. M. S. Weiss, private communication.
19. K. Boyer, T. S. Luk, and C. K. Rhodes, "Possibility of Optically Induced Nuclear Fission," Phys. Rev. Lett. 60, 557 (1988).
20. M. H. R. Hutchinson, I. A. McIntyre, G. N. Gibson, and C. K. Rhodes, "Measurements of 248 nm, Subpicosecond Pulse Durations by Two-Photon Fluorescence of Xenon Excimers," Opt. Lett. 12, 102 (1987).
21. M. D. Dawson, T. F. Boggess, D. W. Garvey, and A. L. Smirl, "A Hybridly Mode-Locked CW Dye-Laser with Brewster Prisms," Opt. Commun. 60, 79 (1986).
22. K. S. Budil, I. A. McIntyre, and C. K. Rhodes, "Cavity Considerations in Hybridly Mode-Locked Femtosecond Dye Lasers," Opt. Commun. 64, 279 (1987).
23. S. Szatmári, F. P. Schäfer, E. Müller-Horsche and W. Mückenheim, "Hybrid Dye-Excimer Laser System for the Generation of 80 fs, 900 GW Pulses at 248 nm," Opt. Commun. 63, 305 (1987).
24. T. S. Luk, U. Johann, H. Egger, H. Pummer, and C. K. Rhodes, "Collision-Free Multiple Photon Ionization of Atoms and Molecules at 193 nm," Phys. Rev. A32, 214 (1985).
25. U. Johann, T. S. Luk, H. Egger, and C. K. Rhodes, "Rare-Gas Electron-Energy Spectra Produced by Collision-Free Multiquantum Processes," Phys. Rev. A34, 1084 (1986).
26. T. S. Luk, T. Graber, H. Jara, U. Johann, and C. K. Rhodes, "Subpicosecond Ultraviolet Multiphoton Electron Spectroscopy of Rare Gases", J. Opt. Soc. B 4, 847 (1987).
27. P. Lambropoulos, "Mechanisms for Multiple Ionization of Atoms by Strong Pulsed Lasers," Phys. Rev. Lett. 55, 2141 (1985).
28. K. Boyer and C. K. Rhodes, "Atomic Inner-Shell Excitation Induced by Coherent Motion of Outer-Shell Electrons," Phys. Rev. Lett. 54, 1490 (1985).
29. A. Szöke and C. K. Rhodes, "Theoretical Model of Inner-Shell Excitation by Outer-Shell Electrons," Phys. Rev. Lett. 56, 720 (1986).

30. G. Wendin, L. Jönsson, and A. L'Huillier, "Screening Effects in Multielectron Ionization of Heavy Atoms in Intense Laser Fields," *Phys. Rev. Lett.* **56**, 1241 (1986).
31. K. Boyer, G. Gibson, H. Jara, T. S. Luk, I. A. McIntyre, A. McPherson, R. Rosman, J. C. Solem, and C. K. Rhodes, "Corresponding Aspects of Strong-Field Multiquantum Processes and Ion-Atom Collisions," *IEEE Transactions on Plasma Science*, in press.
32. K. Boyer, H. Jara, T. S. Luk, I. A. McIntyre, A. McPherson, R. Rosman, J. C. Solem, and C. K. Rhodes, "Discussion of the Role of Many-Electron Motions in Multiphoton Ionization and Excitation," in *Multiphoton Processes*, edited by S. J. Smith and P. L. Knight (Cambridge University Press, Cambridge, 1988) p. 58.
33. L. V. Keldysh, "Ionization in the Field of a Strong Electromagnetic Wave," *Sov. Phys.-JETP* **20**, 4 (1965).
34. Yu. P. Raizer, "Breakdown and Heating of Gases Under Influence of a Laser Beam," *Sov. Phys.-USP* **8**, 650 (1966).
35. MCR Technology Corporation Final Report, Contract No. 9-L46-Z0347-1, 26 September 1986.
36. H. Winter, "Production of Multiply Charged Ions for Experiments in Atomic Physics," in Atomic Physics of Highly Ionized Atoms, Nato ASI Series, Vol. **B96**, edited by Richard Marrus (Plenum Press, New York, 1983) p. 455.
37. R. J. Fortner, private communication.
38. L. Armstrong, Jr., "Relativistic Effects in Highly Ionized Atoms," in Structure and Collisions of Ions and Atoms, edited by I. A. Sellin (Springer-Verlag, Berlin, 1978) p. 69; Atomic Physics of Highly Ionized Atoms, edited by R. Marrus, Nato ASI Series, Vol. **B96** (Plenum Press, New York, 1983).
39. G. A. Chandler, D. D. Dietrich, M. H. Chen, R. J. Fortner, C. J. Hailey, and M. E. Stewart, "Observations of Two-Electron-Jump, Core-Changing X-Ray Transitions in Fluorinelike and Oxygenlike Lanthanum," *Phys. Rev. Lett.* **61**, 1186 (1988).
40. M. S. Pindzola, "Relativistic Effects on Giant Resonances in Electron-Impact Double Ionization," *Phys. Rev.* **A35**, 4548 (1987).
41. E. Källne and J. Källne, "X-Ray Spectroscopy Studies of Atomic Processes in High Temperature Plasmas," in Atomic Physics 10, edited by H. Narumi and I. Shimamura (North-Holland, Amsterdam, 1987) p. 395.
42. H. R. Griem, "Line Profiles of Soft-X-Ray Laser Gain Coefficients," *Phys. Rev.* **A33**, 3580 (1986).
43. D. D. Burgess, D. Everett, and R. W. Lee, "Suppression of Doppler Broadening

- for XUV Transitions in Dense Plasmas," J. Phys. B 12, L755 (1979).
44. W. B. Mori, C. Joshi, J. M. Dawson, D. W. Forslund, and J. M. Kindel, "Evolution of Self-Focusing of Intense Electromagnetic Waves in Plasma," Phys. Rev. Lett. 60, 1298 (1988).
 45. G.-Z. Sun, E. Ott, Y. C. Lee, P. Guzdar, "Self-Focusing of Short Intense Pulses in Plasmas," Phys. Fluids 20, 526 (1987).
 46. Ya. L. Bogomolov, S. F. Lirin, V. E. Semenov, and A. M. Sergeev, "Ionization Self-Channelling of Extremely Intense Electromagnetic Waves in a Plasma," Pis'ma Zh. Eksp. Teor. Fiz. 45, 532 (1987) [Engl. transl.: Sov. Phys. - JETP Lett. 45, 680 (1987)].
 47. J. C. Solem, T. S. Luk, K. Boyer, and C. K. Rhodes, "X-Ray Amplification with Charge-Displacement Self-Channelling," Phys. Rev. Lett., submitted.
 48. P. L. Kelley, "Self-Focusing of Optical Beams," Phys. Rev. Lett. 15, 1005 (1965).
 49. L. I. Schiff, "Measurability of Nuclear Electric Dipole Moments," Phys. Rev. 132, 2194 (1963).

VI. APPENDICES

Appendix A: "Kinetic Energy Distributions of Ionic Fragments Produced by Subpicosecond Multiphoton Ionization of N_2 "

KINETIC ENERGY DISTRIBUTIONS OF IONIC
FRAGMENTS PRODUCED BY SUBPICOSECOND MULTIPHOTON
IONIZATION OF N_2^*

K. Boyer, T. S. Luk, J. C. Solem[†], and C. K. Rhodes

Laboratory for Atomic, Molecular, and Radiation Physics
Department of Physics, University of Illinois at Chicago
P. O. Box 4348, Chicago, Illinois 60680

ABSTRACT

A study of the kinetic energy distributions of ionic fragments produced by subpicosecond irradiation of N_2 with 248 nm radiation at an intensity of $\sim 10^{16}$ W/cm² is reported. These measurements, in comparison to other findings involving molecular excitation with charged particles and soft x-rays, reveal several important features of the nonlinear coupling. Four ionic dissociative channels are identified from the data on the multiphoton process. They are $N_2^{2+} \rightarrow N^+ + N^+$, $N_2^{2+} \rightarrow N + N^{2+}$, $N_2^{3+} \rightarrow N^+ + N^{2+}$, and $N_2^{3+} \rightarrow N^+ + N^{3+}$, three of which are charge asymmetric. The data for the energy distributions are found to be in approximate conformance with a simple picture involving ionizing transitions occurring within a time of a few cycles of the ultraviolet wave at a nearly fixed internuclear separation close to that of the ground state $X^1\Sigma_g^+$ molecule. The implication follows that a strong nonlinear mode of coupling is present which causes a high rate of energy transfer. A simple hypothesis is presented which unites the ability for rapid energy transfer with the observed tendency to produce charge asymmetric dissociation.

* resubmitted to Physical Review A, 19 September 1988

† present address: Theoretical Division MS-B210, Los Alamos National Laboratory, Los Alamos, NM 87545

I. INTRODUCTION

Processes involving the rapid production of molecular vacancies generally result in energetic fragmentation of the molecular ion produced. In particular, studies have been made of the fragmentation of N_2 , having the ground state configuration $(1\sigma_g)^2(1\sigma_u)^2(2\sigma_g)^2(2\sigma_u)^2(1\pi_u)^4(3\sigma_g)^2$, arising from photon-induced inner-shell excitation,¹⁻³ electron collisions,⁴ and ion collisions.⁵ Rapid molecular ionization by multiphoton processes is also expected to produce ionic fragments with a characteristic distribution of kinetic energies.⁶⁻⁸ Comparison of the energy spectra of the fragments produced by these different means can give information on the corresponding mechanisms of vacancy formation and the dynamics of molecular dissociation. The present study discusses the observation of N^+ , N^{2+} , and N^{3+} fragments produced by multiphoton ionization of N_2 with subpicosecond 248 nm radiation at an intensity of $\sim 10^{16}$ W/cm². These data reveal specific information on the dynamics of these nonlinear molecular events.

Assuming that the molecular potential is dominated by the coulomb term, the time τ for two atoms, with a reduced mass of M initially situated at a bond distance of $\sim 2\beta a_0$ and ionized suddenly by a pulse of radiation to charge states Z_1 and Z_2 , to undergo a coulomb explosion^{1,9,10} and develop a separation of x , is

$$\tau = \frac{\lambda_c}{c\alpha^2} \sqrt{\frac{\beta^2 M}{2m_e Z_1 Z_2}} \left[\frac{x\sqrt{1 - 2\beta a_0/x}}{2\beta a_0} + \frac{1}{2} \ln \left(\frac{1 + \sqrt{1 - 2\beta a_0/x}}{1 - \sqrt{1 - 2\beta a_0/x}} \right) \right]. \quad (1)$$

In Eq. (1) α is the fine structure constant, m_e the electron mass, λ_c the electron Compton wavelength, a_0 the Bohr radius, and c the speed of light. For $x = 1.0$ nm, with $M = 7$ amu, $\beta = 1$, $Z_1 = 2$, and $Z_2 = 1$, Eq. (1) gives $\tau = 14.6$ fs. For these parameters, the explosion of a homonuclear diatomic molecule would yield an ion kinetic energy of $U_0 = 13.6$ eV for each fragment, a magnitude that can be

readily measured. In particular, this suggests that information on electron ionization rates in the femtosecond range associated with the production of the multiply charged ions can be obtained from the kinetic energy distributions of the ionic spectra.⁶⁻⁸

II. EXPERIMENTAL CONSIDERATIONS

In these studies of ion spectra, a subpicosecond 248 nm source¹¹ was used to produce the ionization in a small focal volume under collision-free conditions and the energies of the ions were measured in a time-of-flight spectrometer.¹² In the apparatus for ion detection,¹³ the particles were extracted through a 0.5 mm aperture by a static field of 100 V/cm. An additional potential of 1.3 kV was applied to the ions before entering the 1 m long free-drift region.

Several factors can contribute to the observed energy resolution of the ion signals.¹⁴ In order to isolate the effect arising from molecular dissociation, the experiments were performed in a regime for which (1) the density was sufficiently low so that the space charge energy was small and (2) the ion energy was sufficiently high so that the expansion of the ion packet during its flight to the detector was negligible.¹⁴ The proper conditions were established by a study of the resolution obtained for atomic Ar, a species for which the contribution from dissociation is absent. Although the resolution limit arising from the space charge effect deduced from the N_2^+ data was approximately 0.13 eV for our experimental conditions, the actual value was somewhat greater, since the main source of energy spreading for the energetic ions was due to the time dispersion characteristic of this technique. For 6 eV N^+ ions in our apparatus, the time dispersion is calculated to be 9.6 ns/eV. This figure, together with the electronic width of 5 ns, gives an energy resolution of ~ 0.5 eV. Similarly, resolutions of 1.4 eV and 3.0 eV are obtained for 10 eV N^{2+} and 20 eV N^{3+} ions, respectively. Furthermore, the absolute energy

scale is governed by the ability to determine accurately the arrival time corresponding to zero-initial-energy ions. These considerations result in experimental ion energy resolutions of ~ 1 eV for 6 eV N^+ , ~ 2.8 eV for 10 eV N^{2+} , and ~ 6 eV for 20 eV N^{3+} .

III. EXPERIMENTAL FINDINGS AND DISCUSSION

The time-of-flight data for the N^+ ion signal are illustrated in Fig. (1a). Two peaks displaced symmetrically about a central component are clearly observed. Analysis of this signal shows that the prominent central feature comes from ions with a very low kinetic energy and that the two symmetrically placed components correspond to the energetic fragments generated by the molecular dissociation. This is readily seen from comparison of the data in Fig. (1a) with that shown in Fig. (1b) for N_2^+ , an ion which should exhibit only a central thermal energy peak, perhaps involving some additional broadening arising from the effect of space charge. The two symmetrically located components of dissociative origin exhibited in Fig. (1a) result from two velocity groups of ions, one initially headed toward the detector and a corresponding oppositely directed component whose momentum is reversed by the action of the extracting field.^{2,15} Analyses of these peaks for N^+ , N^{2+} , N^{3+} has been used to determine both (a) the relative abundances and (b) the distributions of kinetic energies arising from the molecular fragmentation.

Integrated over all energies, the relative abundances in percent are 54, 32, and 14 for N^+ , N^{2+} , and N^{3+} , respectively. Interestingly, the ratio $N^+/N^{2+} \approx 1.7$, a value not far from the minimum magnitude seen (~ 1.9) in the soft x-ray studies¹ slightly above the nitrogen K-edge ($\hbar\omega = 440$ eV), but rather far from that observed (~ 4.7) well beyond the K-edge ($\hbar\omega = 930$ eV) in other work.⁹ A considerably higher fraction of N^{2+} appears to be produced by the multiphoton mechanism for the conditions of these experiments.

The distributions of the kinetic energies for multiphoton produced N^+ and N^{2+} ions can be compared to the corresponding distributions observed in the soft x-ray studies.¹⁻³ Figure (2) illustrates this comparison for N^+ ions which, for the x-ray work, arise from the



channel. All three distributions shown in Fig. (2) have their maximum strengths in the $\sim 3.9 - 5.0$ eV range. Essentially, the same result is found in experiments involving electron⁴ and ion collisions.⁵ Since the energy resolution of the multiphoton data is not sufficient to exhibit the structure seen in the data produced in the x-ray studies, no significance can be attached to absence of those structured features in the multiquantum result. Overall, therefore, the gross character of the spectrum of the N^+ ions produced does not depend strongly on the mechanism of ionization. X-rays, electrons, ions, and multiphoton coupling all produce N^+ ions of approximately the same energy.

Ranked in order of ascending binding energy, the outer molecular orbitals of N_2 , based on the spectroscopy¹⁶⁻¹⁸ of N_2 and N_2^+ , are $1\pi_u$, $3\sigma_g$, $2\sigma_u$, and $2\sigma_g$ with values of ~ 15.6 eV, ~ 16.7 eV, ~ 18.7 eV, and ~ 38 eV, respectively. Consequently, these four orbitals represent two approximately separate scales of excitation with the $1\pi_u$, $3\sigma_g$, and $2\sigma_u$ being the lowest, and the $2\sigma_g$ highest.

For the channel producing the N^+ ions observed, the N_2^{2+} valence holes leading to dissociation appear to be primarily of $^1\Delta_g[1\pi_u^{-2}]$ character,^{19,20} the lowest energy two-hole configuration. Since the KVV Auger process associated with the x-ray excitation occurs on a time short compared to molecular nuclear motions, the internuclear separation r_0 of the nascent N_2^{2+} system is expected to be very near to that given by the $N_2 X^1\Sigma_g^+$ ground state ($r_0 = 1.098$ Å). Therefore, the agreement of the N^+ fragment energies suggests that the multiphoton transition

occurs at an internuclear separation close to the same value of r_0 . Low lying metastable states^{21,22} of N_2^{2+} are presumably also formed from the decay which could account for the N^+ generation in the energy range ~ 2 eV.

The dominance of the $1\pi_U^{-2}$ configuration of N_2^{2+} produced by the multiquantum process is not unexpected, since it represents a rather low ionization energy and can be reached by either a direct path from $N_2 X^1\Sigma_g^+$ or a sequential mechanism involving the stable electronically excited $N_2^+ A^2\Pi_U$ state which has a $1\pi_U$ hole. A sequential mechanism proceeding through the lowest ion level, $N_2^+ X^2\Sigma_g^+$, to a $1\pi_U^{-2}$ configuration is considered unlikely, since the $X^2\Sigma_g^+$ state has a $3\sigma_g$ hole.^{16,23} The change in the equilibrium internuclear separation of ~ 0.08 Å between the N_2X and N_2^+A states is sufficiently small to have a negligible effect on the observed kinetic energy distributions for the energy resolution used in these studies.

The production of N^{2+} ions can be considered in a similar light. In this case, the agreement represented in Fig. (2) between the x-ray-produced and multiphoton-generated N^+ distributions does not occur with respect to the corresponding N^{2+} kinetic energy distributions, if it is assumed that the ions arise only from the



channel. The data illustrating this comparison, which includes a fiducial signal arising from Ar^{6+} , are shown in Fig. (3). Roughly, the x-ray and multiphoton data agree for energies above ~ 10 eV, but deviate significantly otherwise. A substantial component of the multiphoton generated ion signal is shifted to a considerably lower energy. Indeed, a prominent peak in the N^{2+} spectrum stemming from the nonlinear coupling is present at 6 – 7 eV, an energy range well below the lower limit of the soft x-ray produced particles.

The maximum exhibited in the 6 – 7 eV range in Fig. (3) for the multiquantum-

produced N^{2+} ions, however, is consistent with formation by the reaction



a channel that is associated with a major feature of the Auger spectrum² of N_2 corresponding to a two-hole binding energy in the vicinity of ~ 70 eV. Indeed, in that region, the only decay channel observed² was process (3) with a characteristic N^{2+} energy of 6.7 ± 1 eV. The N_2^{2+} states implicated,^{2,20} as noted in the x-ray studies,² are ${}^1\Sigma_g[2\sigma_g^{-1}, 3\sigma_g^{-1}]$, ${}^1\Sigma_u[2\sigma_g^{-1}, 2\sigma_u^{-1}]$, and ${}^1\Pi_u[2\sigma_g^{-1}, 1\pi_u^{-1}]$. Furthermore, in those studies, spin conservation requires fragmentation from those singlet hole configurations to excited products. The likely final states are $N^{2+}({}^2P^o) + N({}^2D^o)$, $N^{2+}({}^2P^o) + N({}^2P^o)$, and $N^{2+}({}^4P) + N({}^4S^o)$. The multiphoton data are consistent with approximately equal participation of these three channels.

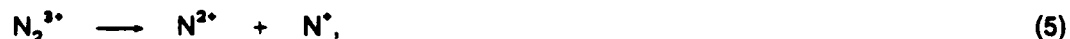
In parallel with the discussion of process (2) above, the N_2^{2+} system could be produced either by a direct mechanism from N_2 $X^1\Sigma_g^+$ or by a sequential mechanism involving states of N_2^+ . Since $N_2^+(X)$ and $N_2^+(A)$ have $3\sigma_g$ and $1\pi_u$ holes, respectively, the production of the $N_2^{2+} {}^1\Sigma_g^+$ and the $N_2^{2+} {}^1\Pi_u$ levels given above could involve a sequential mechanism with X and A first ion states serving as intermediate species. However, on the basis of the molecular configurations, the participation of the ${}^1\Sigma_u[2\sigma_g^{-1}, 2\sigma_u^{-1}]$ state by a sequential process would not be expected to occur through the X and A states. Presumably, this would require the generation of significantly more highly excited N_2^+ levels, such as the $N_2^+ B^2\Sigma_u^+$ which involves a $2\sigma_u$ hole.

The neutral nitrogen atoms produced by process (4) would escape detection, but a fraction of them would be expected to be converted to N^+ after dissociation by subsequent multiphoton ionization in the focal zone. The presence of such a group of 6 - 7 eV N^+ ions would, therefore, contribute to the signal in that range shown in Fig. (2). Since the overall N^+/N^{2+} ratio is significantly greater

than unity, this component of the N^+ signal is expected to be relatively small in comparison to those produced by process (2).

Alternatively, since the high energy region of the N^+ kinetic energy distribution overlaps the low energy region of the N^{2+} distribution, the N^{2+} seen in the 6 - 7 eV range could, in principle, be produced entirely by a velocity selective conversion by multiquantum ionization of N^+ to N^{2+} . Although the multiphoton data cannot rule out this possibility, the general agreement of the N^+ and N^{2+} distributions with the corresponding ones observed in the synchrotron studies diminishes the likelihood that such a selective conversion is playing a dominant role.

A distinct group of N^{2+} ions is apparent in Fig. (3) in the 11 - 14 eV region for both the multiquantum and synchrotron^{2,3} studies. The observation of N^{2+} with kinetic energies in the 11 - 14 eV range cannot plausibly be associated with channels in either N_2^+ or N_2^{2+} , even with allowance for a second step of ionization (e.g., $N^+ \rightarrow N^{2+}$) occurring after the act of molecular dissociation. The curves for these two species are simply not steep enough to give a sufficient impulse.^{16,19,20} A more highly charged system, presumably N_2^{3+} , which can undergo the reaction



is indicated. This, of course, is in agreement with the findings of the x-ray studies.³

For N_2^{3+} , the coulomb term is expected to dominate the molecular curve, with the exception of relatively minor molecular contributions for internuclear separations in the $\sim 1 \text{ \AA}$ range. The coulombic N_2^{3+} curve indicated in Fig. (4) shows that its position is consistent with the magnitude of the observed N^{2+} kinetic energies for a vertical excitation of the system in the potential energy region $\sim 84 \text{ eV}$. Furthermore, within the experimental resolution ($\sim 3 \text{ eV}$), the 11 - 14 eV range agrees well with the observed N^{2+} energy ($\sim 13 \text{ eV}$) in the soft x-ray studies² stemming, in that case, from N_2^{3+} formation arising from a $2\sigma_g^{-2}$

level with the assumption of an additional shake-off from the first Auger event.

Overall, the observed N^* and N^{2*} distributions, assuming that the ions arise from the decay channels $N^* + N^*$, $N^{2*} + N$, and $N^{2*} + N^*$, all appear consistent with vertical excitation of the N_2 system to corresponding N_2^{2*} and N_2^{3*} configurations. It is also known¹⁷ that the ionic ground and low lying N_2^* levels ($X^2\Sigma_g^+$, $A^2\Pi_u$, and $B^2\Sigma_u^+$) all have equilibrium internuclear separations very close to the neutral N_2 ground state $X^1\Sigma_g^+$. Therefore, the removal of one electron from the neutral molecule does not cause appreciable nuclear motion or displacement. Excitation to higher charge states, however, such as N_2^{2*} and N_2^{3*} , generally leads to unstable levels which will cause rapid motion of the nuclei. Since N_2 and N_2^* are stable with $r_{N_2} \approx r_{N_2^*}$, the present multiphoton data do not give information on the removal of the first electron. However, the observation of dissociative channels from N_2^{2*} and N_2^{3*} enables an estimate to be made concerning the dynamics of electron removal involving those systems.

Consider the production of N_2^{3*} from N_2^* by the sequential mechanism



in which m_1 and m_2 denote the number of ultraviolet quanta involved. The observed absence of appreciable nuclear motion in the formation of N_2^{3*} can be used to estimate a residence time τ for the unstable N_2^{2*} system. This gives an approximate figure for the electron emission rate for the physical regime being studied. For this estimate we will assume that the N_2^{2*} and N_2^{3*} molecular curves are dominated by the coulombic interactions corresponding to $N^* + N^*$ and $N^{2*} + N^*$, respectively. In this picture, the net change in the kinetic energy $\Delta\phi$ of the N^{2*} fragment produced by process (5) arising from a small displacement Δr in the N_2^{2*} ($N^* + N^*$) system can be simply represented by

$$\Delta\phi = \frac{e^2}{r_0} - \frac{e^2}{r_0 + \Delta r} \quad (8)$$

in which r_0 the initial internuclear distance. The data indicate that

$$r_0 = r_{N_2} = r_{N_2^+} = 1.1 \text{ \AA}. \quad (9)$$

The magnitude of Δr can be derived from Eq. (8) by equating $\Delta\phi$ with the shift observed in the N^{2+} energies between the synchrotron data² and the multiphoton results arising from the $N^{2+} + N^+$ decay. Since no shift was observed, we use the experimental energy resolution $\Delta\epsilon$ of N^{2+} to establish an upper bound Δr_m on this displacement. The result is

$$\Delta r_m \leq r_0 \left(\frac{1}{e^2/(r_0\Delta\epsilon) - 1} \right) \quad (10)$$

which, with $\Delta\epsilon = 3 \text{ eV}$, gives $\Delta r_m \leq 0.33 \text{ \AA}$. The corresponding upper bound on the residence time τ_m of the N_2^{2+} system can be evaluated from Eq. (1) with $Z_1 = Z_2 = 1$, the parameter β selected so that

$$2\beta a_0 = r_0, \quad (11)$$

and

$$x = r_0 + \Delta r_m. \quad (12)$$

This gives $\beta = 1.04$, $x = 1.43 \text{ \AA}$ and yields

$$\tau_m \approx 2.35 \text{ fs}, \quad (13)$$

an interval that is only three periods of the 248 nm wave. Therefore, the ion energy distributions indicate that the lifetime of the N_2^{2+} species, as an intermediate in the production of N_2^{3+} from lower charge states (N_2 or N_2^+), is on the order of or less than approximately three cycles of the wave.

A substantial signal of N^{3+} ions was detected with the peak in the distribution occurring at $\sim 20 \text{ eV}$ as shown in Fig. (5). If we assume that the channel producing these ions is



and further assume that the ionization occurs at the internuclear separation implied by the production of the N^+ and N^{2+} species, the energy of the N^{3+} fragment would be exactly 3/2-fold the energy of the N^{2+} ion produced in the $N^{2+} + N^+$ reaction. Given the peak at ~ 12.8 eV for N^{2+} shown in Fig. (3), the expected N^{3+} kinetic energy is ~ 19.1 eV, a value very close to the measured maximum of the distribution at ~ 20 eV and indistinguishable from it with the experimental resolution pertaining to this measurement.

We note that the N^+ component arising from reaction (14) is expected to be difficult to observe. The fraction of N^+ ions produced in that way is relatively small and any conversion of N^+ to N^{2+} by subsequent ionization would be effectively masked by the Ar^{6+} fiducial signal at ~ 20 eV.

Finally, if N_2^{3+} is regarded as an intermediate in the formation of N_2^{4+} , in parallel with the discussion above concerning N^{2+} ion production following the formation of N_2^{3+} , a maximum residence time comparable to that found for N_2^{2+} in Eq. (13) is found to apply.

Similar reasoning concerning the generation of N^{2+} ions from the N_2^{4+} system would place the corresponding N^{2+} energy at ~ 25 eV, a point for which no signal is evident in the distribution illustrated in Fig. (3). Apparently, the



channel is not dynamically favored under the conditions studied in this work, although clearly energetically accessible, since the $N^{2+} + N^{2+}$ potential lies in Fig. (4) below the corresponding $N^{3+} + N^+$ curve for all values of internuclear separation $r \geq r_0$. Interestingly, reaction (15) has been detected in subpicosecond studies²⁴ involving the use of radiation with a wavelength of ~ 600 nm, a finding pointing to a wavelength sensitivity of these amplitudes and a need for further examination

of their frequency dependence.

IV. CONCLUSIONS

The kinetic energy distributions of atomic nitrogen ions produced from N_2 by multiphoton ionization reveal several characteristics of the nonlinear molecular interaction. In comparison to soft x-ray excitation, which produces the molecular vacancies by Auger cascade and shake-off, the final configurations of the valence shell holes produced by the multiphoton and soft x-ray excitation appear to have many similarities.

The observed kinetic energy distributions of the N^+ , N^{2+} , and N^{3+} ions produced by the multiphoton mechanism all find a consistent explanation if it is assumed that the molecular ionization for all species occurs at an internuclear separation close to the equilibrium value for neutral N_2 . Namely, the transitions appear to occur nearly vertically. This finding enables an estimate of the effective residence time of intermediate molecular ionic states to be made with the outcome that this interval has an upper bound on the order of a few optical cycles for N_2^{2+} and N_2^{3+} . Since most of the deposited energy is associated with the formation of the higher charge states, the implication is that the main energy transfer process, when it occurs in the course of the interaction, proceeds quite rapidly. A peak energy transfer rate on the order of a few milliwatts/molecule is inferred from these results. Therefore, a mechanism for strong coupling is presumably present.

Four molecular decay modes are identified involving molecular ion states with a charge as high as N_2^{3+} . They are, specifically, $N^+ + N^+$, $N + N^{2+}$, $N^+ + N^{2+}$, and $N^+ + N^{3+}$. It is notable that three of these represent charge asymmetric modes and that an energetically available symmetric decay channel ($N^{2+} + N^{2+}$) was apparently not present at a detectable level. The dynamics appear to favor asymmetric channels. We observe that the enhancement of an asymmetric mode,

such as $N + N^{2+}$, is a mechanism tending to cause an increase in the N^{2+}/N^+ fraction, a noted feature of the multiphoton data with respect to comparison with the yields observed in the synchrotron studies.

A simple hypothesis unites the rapid energy transfer leading to vertical molecular transitions with the observed tendency to produce charge asymmetric dissociation. The presence of a large induced dipole arising from a multi-electron motion will enhance the ability of the N_2 system to couple to the field. Such a dipole, however, represents a large asymmetric displacement of charge, a situation that would naturally lead to a corresponding asymmetry in the charge states of the dissociation products. This effect would be expected to be most significant for a situation involving a parallel orientation of the molecular axis along the electric vector of the ultraviolet wave.⁷ In this sense, the observed charge asymmetry of the ionic products is merely a remnant of the induced electronic motions. Interestingly, the driven excursion of a free electron at $\sim 10^{16}$ W/cm² in a 248 nm field is ~ 8.4 Å, a value more than seven times larger than the equilibrium internuclear separation of N_2 . Even with a considerable reduction of the scale of this motion arising from the restoring binding forces in the molecule, a substantial charge displacement of the outer molecular electrons is expected under these conditions. A system behaving in this way does not decide its fate on the basis of the energy scale associated with potential final states, but rather selects the dynamical mode of interaction which favors the strongest coupling. Hints of similar behavior were seen in earlier studies of the atomic number dependence of multiphoton ionization of atoms.²⁵ Consequently, the final states to which such electronic motions are related become prominent in the observed distributions of the ionic products.

V. Acknowledgments

The authors acknowledge fruitful discussions with G. Wendin. This work was supported by the U. S. Office of Naval Research, the U. S. Air Force Office of Scientific Research, the Directed Energy Office and the Innovative Science and Technology Office of the Strategic Defense Initiative Organization, and the National Science Foundation.

VI. REFERENCES

1. W. Eberhardt, J. Stöhr, J. Feldhaus, E. W. Plummer, and F. Sette, "Correlation between Electron Emission and Fragmentation into Ions following Soft-X-Ray Excitation of the N_2 Molecule," *Phys. Rev. Lett.* **51**, 2370 (1983).
2. W. Eberhardt, E. W. Plummer, I.-W. Lyo, R. Carr, and W. K. Ford, "Auger-Electron-Ion Coincidence Studies of Soft X-Ray-Induced Fragmentation of N_2 ," *Phys. Rev. Lett.* **58**, 207 (1987).
3. Norio Saito and Isao H. Suzuki, "Kinetic Energies of Fragment Ions from N_2 Absorbing Soft X-Rays by a Photoion-Photoion Coincidence Technique," *J. Phys. B* **20**, L785 (1987).
4. B. Brehm and G. deFrenes, "Investigation of Ion Pairs from Fast Decay Processes of Doubly-Charged Molecular Ions," *Int. J. Mass Spectrom. Ion Phys.* **26**, 251 (1978).
5. A. K. Edwards and R. M. Wood, "Dissociation of N_2^{2+} Ions into N^+ Fragments," *J. Chem. Phys.* **76**, 2938 (1982).
6. F. J. Frasinski, K. Codling, P. Hatherly, J. Barr, I. N. Ross, and W. T. Toner, "Femtosecond Dynamics of Multielectron Dissociative Ionization Using a Picosecond Laser," *Phys. Rev. Lett.* **58**, 2424 (1987).
7. K. Codling, L. J. Frasinski, P. Hatherly, and J. R. M. Barr, "On the Major Mode of Multiphoton Multiple Ionization," *J. Phys. B* **20**, L525 (1987).
8. C. K. Rhodes, "Ordered Many-Electron Motions in Atoms and X-Ray Lasers," in Proceedings of the NATO Advanced Study Institute on Giant Resonances in Atoms, Molecules, and Solids, J. P. Connerade, J. M. Esteve, and R. C. Karnatak, eds. (Plenum Press, New York, 1987) p. 533.
9. T. A. Carlson and M. O. Krause, "Relative Abundances and Recoil Energies of Fragment Ions Formed from the X-Ray Photoionization of N_2 , O_2 , CO , NO ,

- CO₂, and CF_n," J. Chem. Phys. 56, 3206 (1972).
10. T. A. Carlson and R. M. White, "Measurements of the Relative Abundances and Recoil-Energy Spectra of Fragment Ions Produced as the Initial Consequences of X-Ray Interaction with CH₃I, HI, and DI," J. Chem. Phys. 44, 4510 (1966).
 11. A. P. Schwarzenbach, T. S. Luk, I. A. McIntyre, U. Johann, A. McPherson, K. Boyer, and C. K. Rhodes, "Subpicosecond KrF* Excimer-Laser Source," Opt. Lett. 11, 499 (1986).
 12. W. C. Wiley and I. H. McLaren, "Time-of-Flight Mass Spectrometer with Improved Resolution," Rev. Sci. Instr. 26, 1150 (1955).
 13. T. S. Luk, U. Johann, H. Egger, H. Pummer, and C. K. Rhodes, "Collision-Free Multiple Ionization of Atoms and Molecules at 193 nm," Phys. Rev. A 32, 214 (1985).
 14. T. S. Luk and C. K. Rhodes, "Multiphoton Dissociative Ionization of Molecular Deuterium," Physical Review A, to be published.
 15. W. Eberhardt, E. W. Plummer, C. T. Chen, R. Carr, and W. K. Ford, "New Experiments Using a Soft X-Ray Undulator," Nucl. Instrum. Methods Phys. Res. Sect. A 246, 825 (1986).
 16. A. Lofthus, "The Spectrum of Molecular Nitrogen," J. Phys. Chem. Ref. Data 6, 113 (1977).
 17. K. P. Huber and G. Herzberg, Constants of Diatomic Molecules (Van Nostrand Reinhold Co., New York, 1979).
 18. J. L. Gardner and James A. R. Samson, "Photon and Photoelectron Spectroscopy of CO and N₂," J. Chem. Phys. 62, 1447 (1975).
 19. E. W. Thulstrup and A. Anderson, "Configuration Interacting Studies of Bound, Low-Lying States of N₂⁻, N₂, N₂⁺, and N₂²⁺," J. Phys. B 8, 965 (1975).
 20. H. Ågren, "On the Interpretation of Molecular Valence Auger Spectra," J.

- Chem. Phys. 75 1267 (1981).
21. L. Hellner, M. J. Besnard, G. Dujardin, and Y. Malinovich, "Photoionization Study of Quasibound States of Doubly Charged Molecular Nitrogen Ions," Chem. Phys. 119, 391 (1988).
 22. R. W. Wetmore and R. K. Boyd, "Theoretical Investigation of the Dication of Molecular Nitrogen," J. Phys. Chem. 90, 5540 (1986).
 23. W. E. Moddeman, T. A. Carlson, M. O. Krause, B. P. Pullen, W. E. Bull, and G. K. Schweitzer, "Determination of the K-LL Auger Spectra of N₂, O₂, CO, NO, H₂O, and CO₂," J. Chem. Phys. 55, 2317 (1971).
 24. F. J. Frasinski, private communication.
 25. T. S. Luk, H. Pummer, K. Boyer, M. Shahidi, H. Egger, and C. K. Rhodes, "Anomalous Collision-Free Multiple Ionization of Atoms with Intense Picosecond Ultraviolet Radiation," Phys. Rev. Lett. 51, 110 (1983).

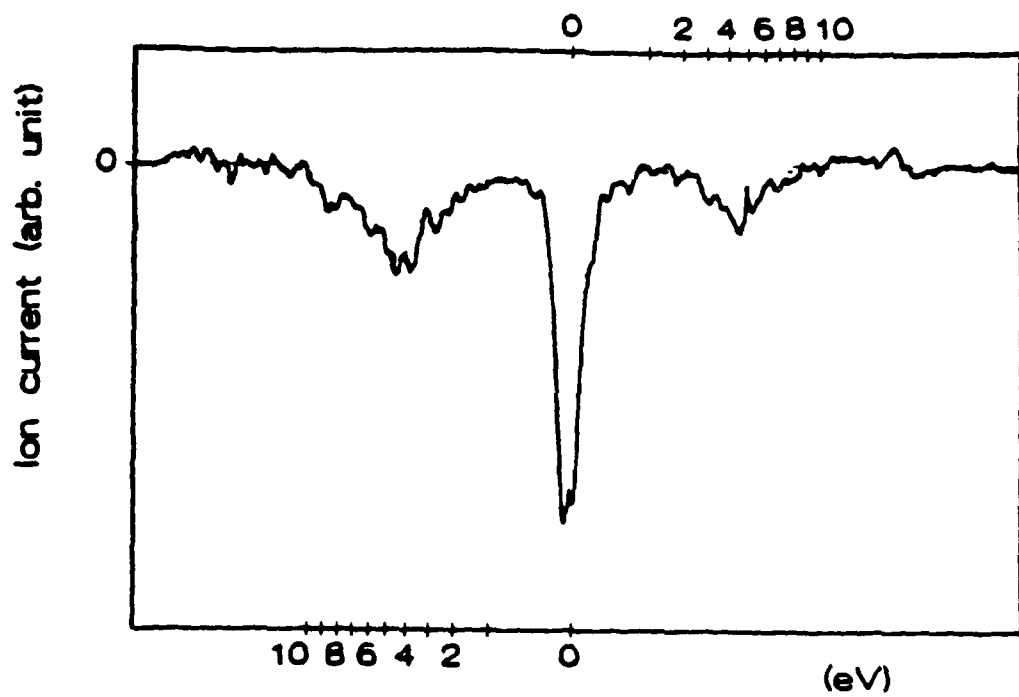
FIGURE CAPTIONS

- Fig. (1): (a) Time-of-flight N^+ ion signal arising from multiphoton ionization of N_2 . The central feature arises from very low energy ions while the two symmetrically located components arise from energetic molecular dissociation from oppositely directed fragments of equal energy. See text for discussion.
- (b) Time-of-flight ion signal corresponding to N_2^+ , a species for which the dissociative components are absent. In this case only a single peak is seen corresponding to the thermal kinetic energy of the parent N_2 molecules.
- Fig. (2): Ion current (N^+) versus ion kinetic energy for N_2 . The + data arise from the multiphoton ionization at 248 nm. The full curve $\text{---}\text{O}\text{---}$ represents the results of Saito and Suzuki [Ref. (3)]. The dashed ---- curve is taken from the results of Eberhardt, et al. [Ref. (1)].
- Fig. (3): Ion current (N^{2+}) versus ion kinetic energy for N_2 . The + data arise from the multiphoton ionization at 248 nm which includes, as a fiducial, a component at ~ 20 eV produced from Ar^{8+} . The solid $\text{---}\text{O}\text{---}$ curve represents the data of Saito and Suzuki [Ref. (3)] and corresponds only to the $N^{2+} + N^+$ channel. General agreement is seen except for the clear peak in the 6 - 7 eV region for the multiphoton data.
- Fig. (4): A partial potential energy diagram of N_2 indicating the ground N_2 $X^1\Sigma_g^+$ and the coulombic contributions to several ionized species. Assuming vertical excitation, the ion energies observed will be one half the amounts indicated for the channels ($N^+ + N^+ - 12.74$ eV; $N^{2+} + N^+ - 25.5$ eV; $N^{3+} + N^+ - 38.2$ eV). The $N^{2+} + N^{2+}$ (51.0 eV) was not observed. See text for discussion.

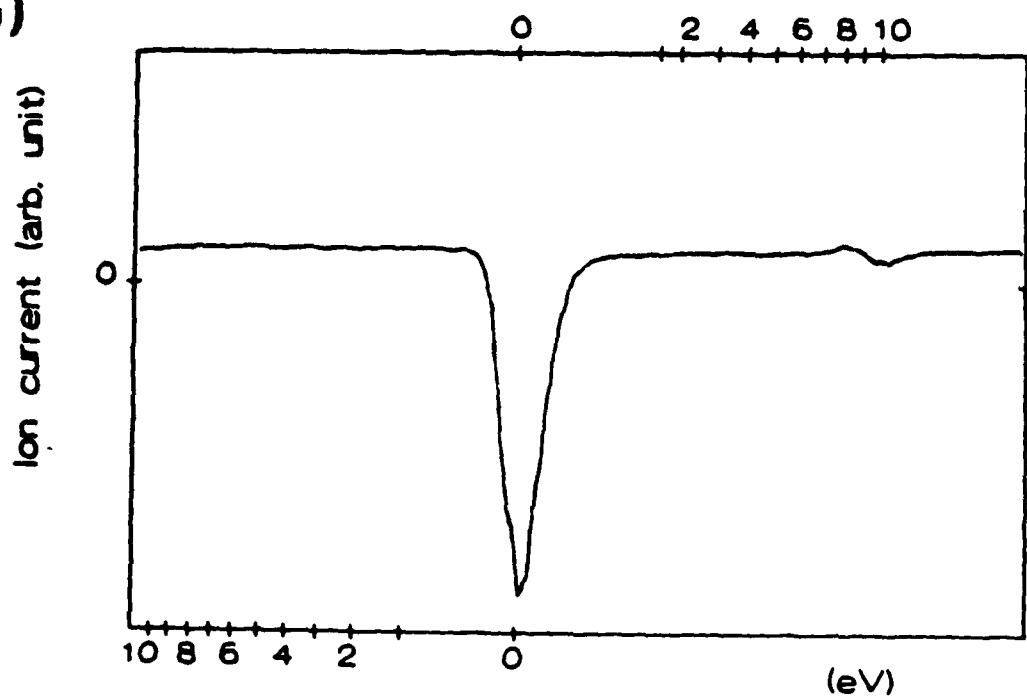
Fig. (5): Ion current (N^{2+}) versus ion kinetic energy for multiphoton ionization of N_2 at 248 nm. A prominent component exists in the 19 – 20 eV region.

(a)

Kinetic energy (away from the detector)



(b)



Kinetic energy (towards the detector)

FIGURE 1

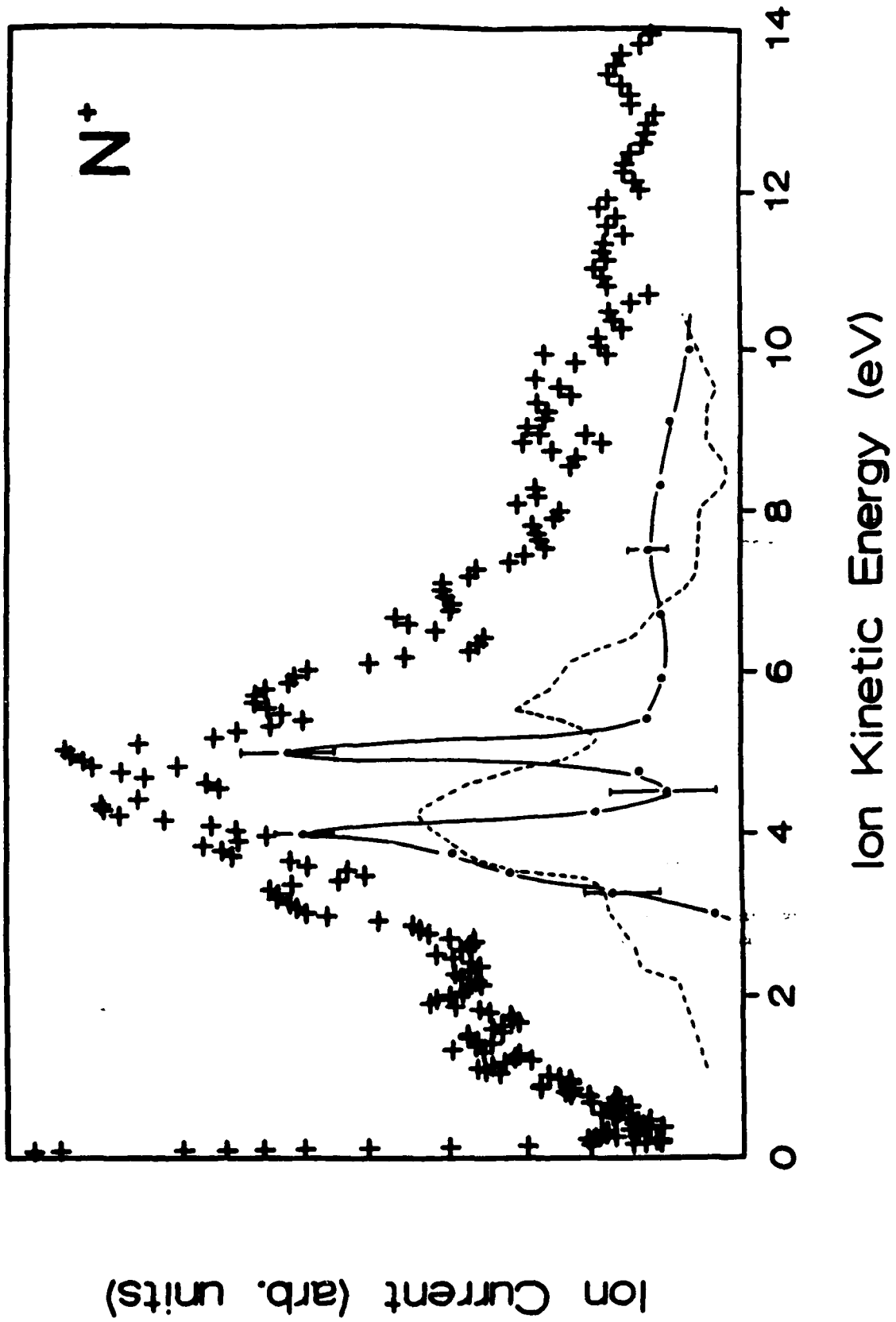


FIGURE 2

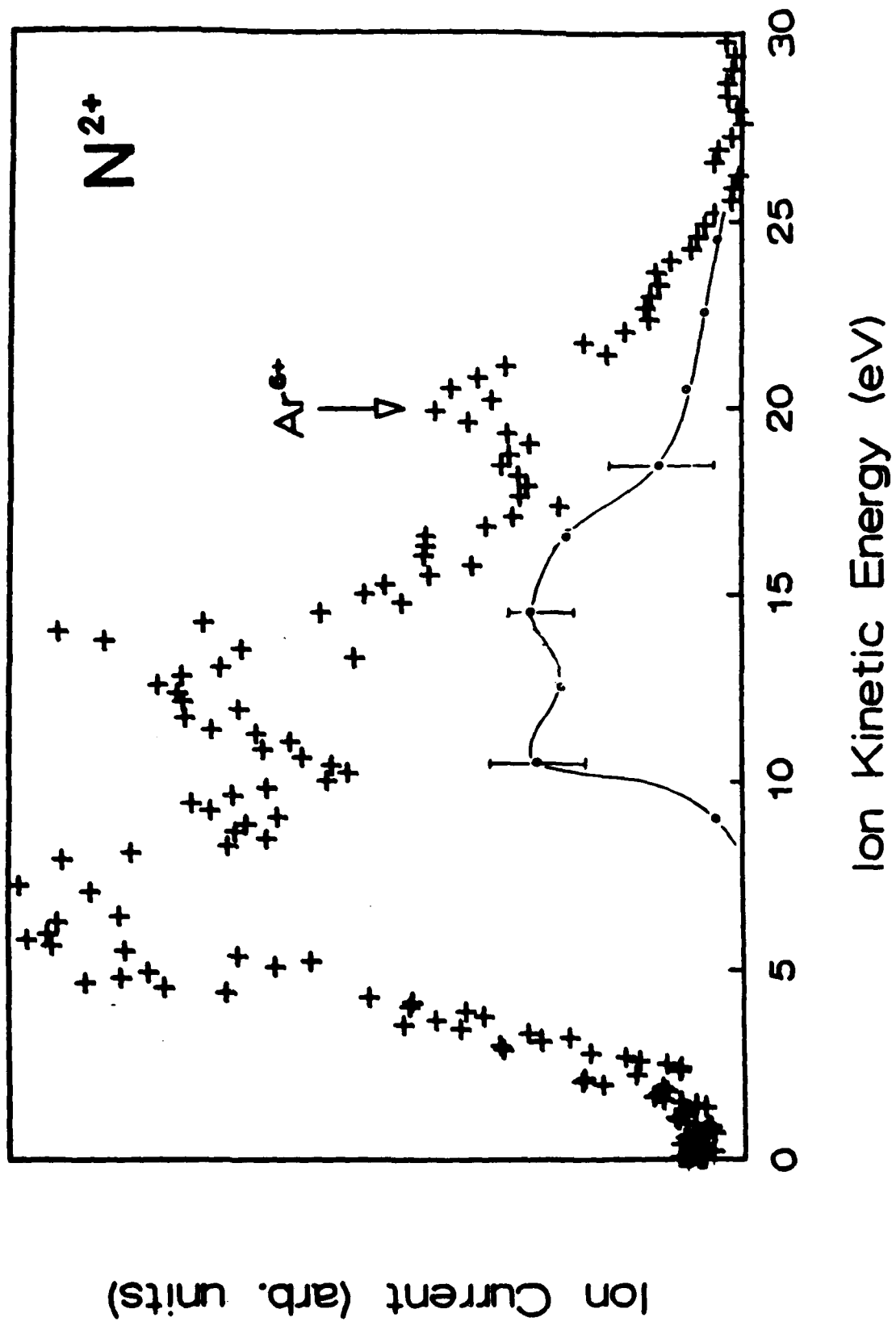


FIGURE 3

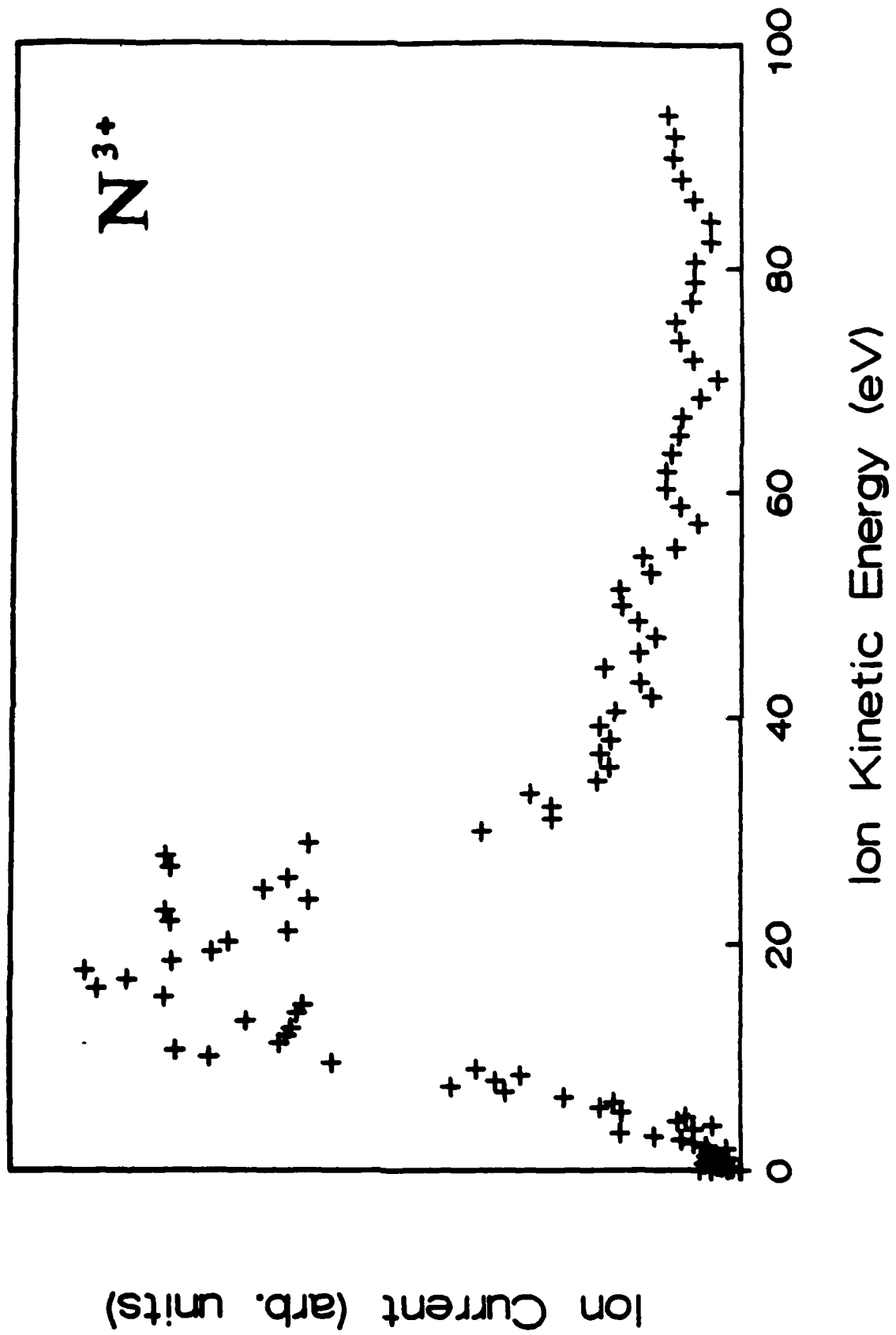


FIGURE 5

Appendix B: "Possibility of Optically Induced Nuclear Fission"

Possibility of Optically Induced Nuclear Fission

K. Boyer, T. S. Luk, and C. K. Rhodes

Laboratory for Atomic, Molecular, and Radiation Physics, Department of Physics,
University of Illinois at Chicago, Chicago, Illinois 60680

(Received 15 June 1987)

The process of nuclear fission induced by nonlinear radiative coupling to atomic electrons is considered. For 248-nm radiation at an intensity of $\approx 10^{21}$ W/cm², highly relativistic currents are produced which can couple to the fission mode of nuclear decay. With irradiation for a time of ≈ 100 fs, the results indicate a fission probability of $\approx 10^{-5}$ for ^{238}U nuclei located at the surface of a solid target, a value several orders of magnitude above the limit of detection.

PACS numbers: 25.85.Ge, 32.80.Wr

Nuclear fission can be induced by electromagnetic interactions involving either photons or charged particles if sufficient energy is communicated to the nucleus enabling the system to penetrate the fission barrier. Known examples of electromagnetically induced fission are photofission,^{1,2}

$$\gamma + A \xrightarrow{\sigma_{\text{eff}}} f_1 + f_2 + \bar{\nu}n, \quad (1)$$

electrofission,³

$$e^- + A \xrightarrow{\sigma_{\text{eff}}} f_1 + f_2 + \bar{\nu}n + e^-, \quad (2)$$

and muon-induced fission.^{4,5} It has also recently been proposed^{6,7} that driven motions of atomic electrons arising from intense irradiation of atoms can couple energy to nuclear transitions occurring between bound nuclear states. This latter mechanism has some features in common with processes of nuclear excitation and deexcitation in which atomic electronic transitions play a role.⁸⁻¹³

The present work examines the possibility of optically induced nuclear fission of heavy elements arising from coupling to driven motions of atomic electrons produced by intense external radiation. The fission process is a particularly favorable one for the demonstration of nuclear excitation. It (1) generally has a large nuclear matrix element, (2) is a broad channel permitting coupling to spectral power over a wide range, and (3) involves a very large energy release comprising distinctive emissions. It will be shown that very large instantaneous fission rates may be generated in a considerable range of nuclear materials. If this can be achieved, extremely bright and spatially localized high-flux pulsed sources of fission fragments, neutrons, and γ radiation could be produced (e.g., $\geq 10^{24}$ fission fragments/cm² s).

The acceleration of electrons to an energy sufficient to surpass the threshold of the fission reaction can be achieved in the focal region of an intense laser pulse.^{14,15} The availability of an ultraviolet laser technology^{16,17} capable of producing subpicosecond pulses with energies approaching the joule level in low-divergence beams at

high repetition rates is making possible a regime of physical study concerning the behavior of matter at extremely high intensities^{18,19} in the 10^{20} - 10^{21} -W/cm² range. Since it can be shown^{14,15} that intensities comparable to 5×10^{19} W/cm² at 248 nm will cause strongly relativistic motions to occur, the use of an intensity of $\approx 10^{21}$ W/cm² would then generate relativistic electrons^{14,15} with an energy sufficient ($\gamma \approx 24$) to produce electrofission by the collisional mechanism represented by reaction (2). We also note that the bremsstrahlung produced collaterally by the fast electrons in the target material can also participate in the production of fissioning material through the photofission reaction (1). The influence of both of these processes is considered below for the case of a solid target composed of ^{238}U .

Extant data²⁰⁻²⁴ on photofission and electrofission of ^{238}U enable a simple estimate to be made of the probability of fission caused by irradiation of material with 248-nm radiation at an intensity of $\approx 10^{21}$ W/cm². The approach used parallels the classical procedure used in an earlier estimate²⁵ of the rate of excitation of atomic inner-shell electrons. We consider a plane solid uranium target with the ultraviolet radiation incident normal to surface. For this estimate, a pulse width with a duration $\tau \approx 100$ fs and a focal area, positioned at the surface, of ≈ 1 μm in diameter are assumed. With the density of solid uranium as ≈ 19 g/cm³, if all of the bound electrons were free and uniformly distributed, the average electron density in the material would be $\rho_e \approx 4.4 \times 10^{24}$ cm⁻³. Since the projected driven motions of these electrons are highly relativistic at an intensity of $\approx 10^{21}$ W/cm², the magnitude of the electronic velocity will be approximated by the speed of light c . Thus, the maximum driven particle current is given by

$$j \approx c\rho_e \approx 1.3 \times 10^{35} \text{ cm}^{-2} \text{ s}^{-1}. \quad (3)$$

The threshold for the electron energy for electrofission in ^{238}U is approximately 10 MeV. Since the electrofission cross section^{21,16} σ_{ef} is in the range of ≈ 1 mb for ^{238}U , the transition rate is $\sim j\sigma_{\text{ef}} \approx 1.3 \times 10^8 \text{ s}^{-1}$ which, for a pulse length τ of $\approx 10^{-13}$ s, gives a total transition prob-

ability for electrofission of

$$P_{ef} \sim j\sigma_{ef}\tau \approx 10^{-5}. \quad (4)$$

From the known systematics of nuclear-fission barrier heights,^{2,26,27} some heavier materials like ^{252}Cf , and particularly certain isomers,²⁸ are expected to have threshold electron energies somewhat less than that characteristic of ^{238}U . However, since the photofission and electrofission processes generally go mainly through the $E1$ giant dipole resonance, a consideration of the sum rule for these transitions^{29,30} suggests that the cross sections for the electrofission process for other heavy materials will not vary more than a factor of 10 from the value corresponding to uranium.

The volume of material involved in this interaction depends upon the depth of penetration of the ultraviolet field into the plasma. Since the critical electron density n_c is $1.6 \times 10^{22} \text{ cm}^{-3}$ at 248 nm, a value more than 200-fold less than the density estimated for the plasma under consideration, the uranium plasma is highly overdense. However, since the driven motion of the electrons is strongly relativistic, the penetration length of the external field has significant relativistic corrections which extend the propagation into the normally forbidden overdense region.³¹ The dielectric constant ϵ for this case can be written as

$$\epsilon = 1 - \frac{\omega_p^2}{\omega^2} \left[1 + \frac{e^2 E_0^2}{m^2 c^2 \omega^2} \right]^{-1/2}. \quad (5)$$

In Eq. (5) ω_p is the customary plasma frequency, E_0 the peak value of the radiative electric field, ω the frequency of the wave, e the electronic charge, and m the mass of the electron. For an intensity of $\approx 10^{21} \text{ W/cm}^2$, ω_p corresponding to a plasma density $\rho_e \approx 4.4 \times 10^{24} \text{ cm}^{-3}$, and ω for 248 nm, the resulting skin depth³² δ for damping of the propagation is $\delta \approx 20 \text{ nm}$. For these conditions, we have ignored collisions and estimate that the electrons have a total energy^{14,15,33} γmc^2 corresponding approximately to $\gamma \approx 24$ and, therefore, experience a change in the relativistic factor $\Delta\gamma \approx 23$ due to the acceleration by the ultraviolet field. This magnitude of $\Delta\gamma$ is consistent with the maximum value that can be achieved by laser acceleration at a given power, regardless of the focusing conditions or the wavelength of irradiation.¹⁵ For our case, in which the total power is $\approx 10^{13} \text{ W}$, the maximum magnitude¹⁵ of $\Delta\gamma$ is $\Delta\gamma_{\text{max}} = 164$.

From the discussion given above, it is possible to estimate the energy of the fission yield that would be generated by irradiation of a solid uranium (^{238}U) surface with a single pulse. The fission yield Y_{ef} corresponding to the electrofission channel can be written as

$$Y_{ef} = \rho_0 A \delta P_{ef} \Delta E_f \quad (6)$$

in which ρ_0 is the uranium atom density, A the focal spot area, δ the skin depth, P_{ef} the electrofission probability,

and ΔE_f the average fission energy. With $\Delta E_f \approx 165 \text{ MeV}$ and the other parameters as discussed above, $Y_{ef} \approx 0.2 \mu\text{J}$, or equivalently, approximately 8400 fission events. A similar outcome would be expected from a ^{232}Th target.³⁴

Since a highly relativistic current of electrons is produced in a dense plasma having ions of a high charge Z by the interaction of the oscillating electrons with the solid target, it is expected that a substantial quantity of energetic bremsstrahlung will be generated, some of which will be in the energy range ($\approx 10 \text{ MeV}$) corresponding to the photofission^{20,21} process (1). Furthermore, since $\sigma_{\gamma f} \sim 10^2 \sigma_{ef}$, the contribution of the photofission channel may not necessarily be negligible. In order to evaluate this contribution, we will assume that the plasma conditions are such that a fraction of $\approx 10^{-3}$ of the incident radiative energy is channeled into energetic bremsstrahlung.^{35,36} For an incident energy of $\approx 1 \text{ J}$, this bremsstrahlung would then account for $\approx 1 \text{ mJ}$, an estimate that is based on the measured scaling of hard x-ray production in studies of fusion plasmas.³⁵ If it is further assumed that all of this bremsstrahlung can participate in the photofission reaction, then $\approx 10^9$ quanta are available. Given the photofission cross section of $\approx 10^{-25} \text{ cm}^2$, this leads to the production of ≈ 50 fissions in the active volume, a value considerably less than that estimated for the electrofission mechanism. However, since the range³⁷ of the bremsstrahlung is $\approx 1 \text{ cm}$ in solid uranium, an additional $\approx 10^6$ fissions would be produced in a much larger region in the material surrounding the focal volume. Of those, only that fraction within the fission-fragment range³⁸ of $\approx 5 \mu\text{m}$ of the surface would produce escaping fission ions. This would be $\approx 10^3$ particles. A major fraction of the neutrons produced ($\approx 10^6$), however, would escape from a sample³⁹ with dimensions comparable to 1 cm. These estimates indicate that the detectable fission-fragment yield may contain a significant contribution from photofission. The total neutron production, however, is probably dominated by the photofission reaction. In terms of the fission yield originating in the focal volume, it seems likely that that would be governed mainly by the electrofission mechanism. Experimentally, a yield of the magnitude estimated, even if reduced by a factor of $\approx 10^3$, could be readily detected.

A substantial quantity of fast uranium ions should be produced by electrostatic acceleration at the surface of the sample. This arises from the tendency of the relativistic electrons to be expelled from the region of high intensity, since the electron trajectories are curved by the magnetic $\mathbf{v} \times \mathbf{B}$ force so that their velocities are nearly parallel with the propagation vector \mathbf{k} of the incident wave.^{14,15} In rough approximation, it appears, for irradiation at $\approx 10^{21} \text{ W/cm}^2$ at 248 nm, that this feature could lead to nearly full expulsion of the electrons from the first skin depth of the focal region, and possibly

somewhat beyond, into a region further below the surface of the solid by the radiation pressure. If we assume complete ionization of the uranium atoms in this surface region, a high and nearly uniform planar charge density is created over a spatial extent of approximately $1 \mu\text{m}^2$. Furthermore, since the heavy uranium ions are inertially confined to positions near their original sites on the surface for a time on the order of ≈ 100 fs, a positively charged ion near this surface will experience a strong electric repulsive force. For sufficiently short times and small distances from the surface, this field E_z is of constant magnitude and directed normally outward from the surface with a value given approximately by

$$E_z \approx \frac{1}{2} \rho_z \quad (7)$$

in which ρ_z is the surface charge density. For fully ionized uranium ($Z=92$) having a lattice constant $r_0 \approx 0.33$ nm, the field E_z is evaluated as

$$E_z = Ze/2r_0^2 \approx 5.9 \times 10^9 \text{ V/cm}. \quad (8)$$

If we further assume that this constant field extends for a distance normal to the surface of ≈ 100 nm, a length roughly one-tenth of the focal spot size, then an ion of charge Z passing through that field will acquire a kinetic energy ϵ_k of approximately

$$\epsilon_k = ZeE_z l. \quad (9)$$

For $Z=92$, ϵ_k is 5.4 MeV with a corresponding kinetic velocity of

$$v_k = (Ze/r_0)(l/M)^{1/2} \quad (10)$$

in which M denotes the mass of a uranium ion. From Eq. (10) we see that a time-of-flight measurement of the ion current would carry direct information on the distribution of charge states formed by the interaction at the surface of the target, a physical parameter directly related to the electrofission rate. An impurity of hydrogen atoms on the surface of the target would make possible a calibration of the scale length l through a measurement of the proton component of the time-of-flight signal.

Earlier work on laser-fusion targets appears to confirm the generation of energetic ions by a surface mechanism of this type. Fast deuterium ions produced from solid CD_2 targets with picosecond irradiation at $1.06 \mu\text{m}$ have been observed⁴⁰ in approximate agreement with Eqs. (9) and (10). For a reasonable choice of parameters ($Z=1$, $l=1 \mu\text{m}$, and $r_0 \approx 2a_0$), Eq. (9) gives $\epsilon_k = 64$ keV, while the measured value⁴⁰ was ≈ 65 keV.

Nuclear fission of heavy elements is predicted to be induced by the irradiation of solid targets with ultraviolet energy at an intensity of $\approx 10^{21}$ W/cm². The fission events should be readily observable through the detection of fast fission fragments, fission neutrons, and γ radiation from excited fission product. For a pulse of ≈ 100 -fs duration, a fission probability of $\approx 10^{-5}$ is estimated for solid ^{235}U . We note that recent calculations⁴¹ of a relat-

ed process involving transitions between bound nuclear states also gives transition probabilities in this general range. Fast highly charged ions of the parent material should also be produced in considerable numbers at the surface. Finally, the ease of detecting single fission events endows this technique with sensitivity to test the character of the atomic response to intense coherent fields, a question of fundamental significance.

This work was supported by the U.S. Office of Naval Research, the U.S. Air Force Office of Scientific Research under Contract No. F49620-85-K-0020, the Innovative Science and Technology Office of the Strategic Defense Initiative Organization, the Lawrence Livermore National Laboratory, under Contract No. 5765705, the National Science Foundation under Grant No. PHY-84-14201, and the Los Alamos National Laboratory under Contract No. 9-X54-C6090-1. Discussions with J. C. Solem are warmly acknowledged. One of us (C.K.R.) also wishes to acknowledge fruitful conversations with J. C. Solem and M. S. Weiss on the fission process.

¹R. O. Haxby, W. E. Shoupp, W. E. Stephens, and W. H. Wells, *Phys. Rev.* **59**, 57 (1941).

²Robert Vandenbosch and John R. Huizenga, *Nuclear Fission* (Academic, New York, 1973), p. 112.

³J. D. T. Arruda-Neto and B. L. Berman, *Nucl. Phys.* **A349**, 483 (1980).

⁴S. Polikanov, in *Dynamics of Nuclear Fission and Related Collective Phenomena*, edited by P. David, T. Mayer-Kuckuk, and A. van der Woude, *Lecture Notes in Physics* Vol. 158 (Springer-Verlag, Berlin, 1982), p. 67.

⁵E. Teller and M. S. Weiss, Lawrence Livermore National Laboratory Report No. UCRL-83616, 1979 (unpublished); E. Teller and M. S. Weiss, in *A Festschrift for Maurice Goldhaber*, edited by G. Feinberg, A. W. Sunyar, and J. Weneser (New York Academy of Sciences, New York, 1980), p. 222.

⁶L. C. Biedenharn, G. C. Baldwin, K. Boyer, and J. C. Solem, in *Advances in Laser Science-1-1985*, edited by W. C. Stwalley and M. Lapp, *AIP Conference Proceedings* No. 146 (American Institute of Physics, New York, 1986), p. 52.

⁷G. A. Rinker, J. C. Solem, and L. C. Biedenharn, Los Alamos National Laboratory Report No. LA-UR-86-4187, 1986 (to be published).

⁸M. S. Freedman, *Annu. Rev. Nucl. Sci.* **24**, 209 (1974).

⁹R. J. Walen and C. Briancon, in *Atomic Inner-Shell Processes*, edited by B. Crasemann (Academic, New York, 1975), Vol. 1, p. 233.

¹⁰D. Kekez, K. Pisk, and A. Ljubičić, *Phys. Rev. C* **34**, 1446 (1986).

¹¹K. Otozai, R. Arakawa, and M. Morita, *Prog. Theor. Phys.* **50**, 1771 (1973).

¹²T. Izawa and C. Yamanaka, *Phys. Lett.* **88B**, 59 (1979).

¹³V. I. Gol'danskii and V. A. Namot, *Yad. Fiz.* **33**, 319

- (1981) [Sov. J. Nucl. Phys. 33, 169 (1981)].
- ¹⁴E. S. Sarachik and G. T. Schappert, Phys. Rev. D 1, 2738 (1970).
- ¹⁵M. J. Feldman and R. Y. Chiao, Phys. Rev. A 4, 352 (1971).
- ¹⁶J. H. Glowina, G. Arjavalingham, P. P. Sorokin, and J. E. Rothenberg, Opt. Lett. 11, 79 (1986).
- ¹⁷A. P. Schwarzenbach, T. S. Luk, I. A. McIntyre, U. Johann, A. McPherson, K. Boyer, and C. K. Rhodes, Opt. Lett. 11, 499 (1986).
- ¹⁸C. K. Rhodes, Science 229, 1345 (1985).
- ¹⁹C. K. Rhodes, in *Giant Resonances in Atoms, Molecules, and Solids*, edited by J.-P. Connerade, J. M. Esteve, and R. C. Karnatak (Plenum, New York, 1987), p. 533.
- ²⁰J. T. Caldwell, E. J. Dowdy, B. L. Berman, R. A. Alvarez, and P. Meyer, Phys. Rev. C 21, 1215 (1980).
- ²¹F. Zamani-Noor and D. S. Onley, Phys. Rev. C 33, 1354 (1986).
- ²²D. H. Dowell, L. S. Cardman, P. Azel, G. Bolme, and S. E. Williamson, Phys. Rev. Lett. 49, 113 (1982).
- ²³H. Stroher, R. D. Fisher, J. Drexler, K. Huber, U. Kniessel, R. Ratzek, H. Ries, W. Wilke, and H. J. Maier, Nucl. Phys. A378, 237 (1982).
- ²⁴K. A. Griffioen, P. J. Countyman, K. J. Knöpfle, K. Van Bibber, M. R. Yearian, J. G. Woodworth, D. Rowley, and J. R. Calarco, Phys. Rev. C 34, 1375 (1986).
- ²⁵C. K. Rhodes, in *Multiphoton Processes*, edited by P. Lambropoulos and S. J. Smith (Springer-Verlag, Berlin, 1984), p. 31.
- ²⁶J. Aschanbach, R. Haeg, and H. Krieger, Z. Phys. A 292, 285 (1971).
- ²⁷J. R. Nix, Annu. Rev. Nucl. Sci. 22, 65 (1972).
- ²⁸R. Vandenbosch, Annu. Rev. Nucl. Sci. 27, 1 (1977).
- ²⁹F. E. Bertrand, Annu. Rev. Nucl. Sci. 26, 457 (1976).
- ³⁰*Giant Multiple Resonances*, edited by F. E. Bertrand (Advanced Academic, New York, 1980).
- ³¹P. Kaw and J. Dawson, Phys. Fluids 13, 472 (1970).
- ³²J. D. Jackson, *Classical Electrodynamics* (Wiley, New York, 1975), 2nd ed.
- ³³L. S. Brown and T. W. B. Kibble, Phys. Rev. 133, A705 (1964).
- ³⁴H. X. Zhang, T. R. Yeh, and Lancman, Phys. Rev. C 34, 1397 (1986).
- ³⁵D. R. Bach, D. E. Casperson, D. W. Forslund, S. J. Gitomer, P. D. Goldstone, A. Hauer, J. F. Kephart, J. M. Kindel, R. Kristal, G. H. Kyrda, K. B. Michell, D. B. Hulsteyn, and A. A. Williams, Phys. Rev. Lett. 50, 2082 (1983); A. Hauer *et al.*, in *Laser Interaction and Related Plasma Phenomena*, edited by H. Hora and G. Miley (Plenum, New York, 1984), Vol. 6, p. 479.
- ³⁶R. A. Grandey, in *Strongly Coupled Plasmas*, edited by G. Kalman and P. Carini (Plenum, New York, 1978), p. 427.
- ³⁷E. L. Chapp, *Gamma Ray Astronomy* (Reidel, Dordrecht, 1976).
- ³⁸U. Littmark and J. F. Ziegler, *Handbook of Range Distributions for Energetic Ions in All Elements* (Pergamon, New York, 1980), Vol. 6, p. 482.
- ³⁹J. R. Stehn, M. D. Golberg, R. Wiener-Chasman, S. F. Mughabghab, B. A. Magurno, and V. A. May, *Neutron Cross Sections*, BNL-325 (Associated Universities, Upton, New York, 1965), Vol. 3, Suppl. No. 2.
- ⁴⁰G. H. McCall, F. Young, A. W. Ehler, J. F. Kephart, and R. P. Godwin, Phys. Rev. Lett. 30, 1116 (1973).
- ⁴¹J. F. Berger, D. Gogny, and M. S. Weiss, Lawrence Livermore National Laboratory Report No. UCRL-96759, 1987 (to be published).

Appendix C: "Measurement of 248-nm, Subpicosecond Pulse Durations by Two-Photon Fluorescence of Xenon Excimers"

those potentials correlating with the $5p^5 ({}^2P_{3/2}) 6p (J = 0)$ atomic state are believed to be repulsive¹¹ so that, at internuclear separations of 0.55 nm, the molecular transition becomes two-photon resonant with the 248.4-nm laser radiation. The molecule will then dissociate along the repulsive potential. Kinetic models of the Xe_2^* system¹² indicate that the population of the excited atomic state that is produced will relax by radiative and collisional processes in a time of ~ 1 nsec to the lowest-lying 0_u^- , 1_u , and 0_u^+ states of the excimer, which then radiate in the VUV at ~ 172 nm. The cross sections for photoionization from the populated atomic states are too small (~ 10 – 18 cm²) to produce significant ionization for laser pulses of ~ 1 -psec duration at intensities of ~ 1 GW/cm², and the relationship between the fluorescence and laser intensities is, therefore, expected to be quadratic and not cubic as was observed in Kr with nanosecond pulses at 248 nm.⁷

Experimental Details

To examine the dependence of the TPF signal on laser intensity, pulses of ~ 1 mJ were taken from a 20-mJ, ultrashort-pulse KrF⁺ laser system⁵ and weakly focused into a stainless-steel cell containing Xe. The VUV fluorescence was filtered by an interference filter (Acton Research Corporation Type 172) and detected with a solar-blind photomultiplier. The variation of the fluorescence intensity with laser intensity was measured over the range $\sim 10^9$ – 10^{10} W/cm² at a gas pressure of 4.5 atm. The results, shown in Fig. 2, indicate a quadratic relationship up to laser intensities of $\sim 3 \times 10^9$ W/cm². Departures at higher intensities may be due to Penning ionization.¹³

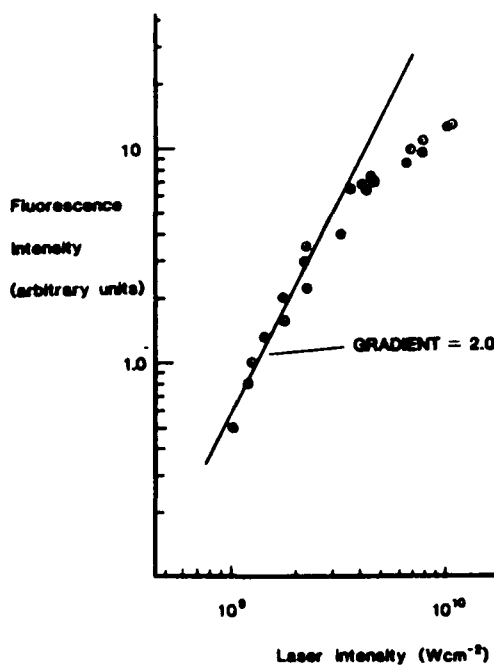


Fig. 2. Experimentally measured dependence of the excimer fluorescence intensity on laser intensity at a gas pressure of 4.5 atm.

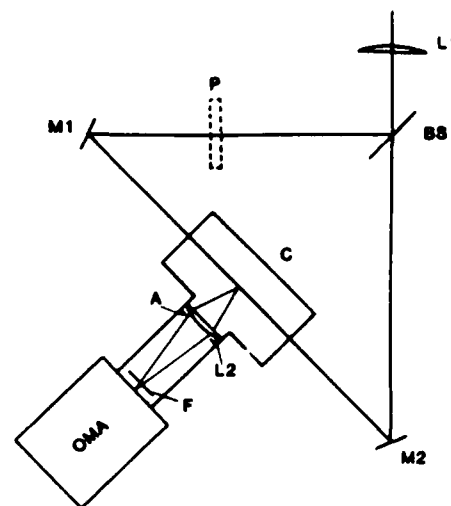


Fig. 3. Experimental arrangement of the two-photon excimer fluorescence autocorrelator.

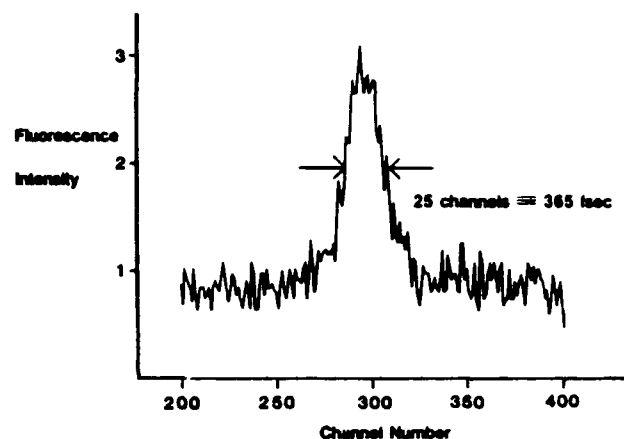


Fig. 4. Measured autocorrelation fluorescence profile for a single subpicosecond KrF⁺-laser pulse.

The experimental arrangement for a TPF autocorrelator using high-pressure Xe as the two-photon absorber is shown in Fig. 3. The 1-mJ pulse is focused weakly by a 1-m focal-length lens (L1), and the pulse is divided into two replicas by the dielectric 50/50 beam splitter (BS). The two counterpropagating pulses are directed into a cell (C) containing Xe by mirrors M1 and M2, and the fluorescence is imaged by a 5.5-cm focal-length LiF lens (L2) through an evacuated tube onto an optical multichannel analyzer (OMA), which has been sensitized for VUV radiation by a film of sodium salicylate deposited upon the entrance end of the fiber-optic coupler. An interference filter (F) with transmission at 172 nm is placed in front of the OMA to remove scattered 248.4-nm laser radiation. The system was calibrated by measuring the shift in the autocorrelation fluorescence pattern when a fused-silica plate (P) of known thickness was introduced into one arm of the triangle.

A fluorescence intensity profile of a pulse, obtained at a pressure of 2 atm and an intensity of $\sim 2 \times 10^9$ W/cm², is shown in Fig. 4 and corresponds to a dura-

tion of 365 fsec, assuming a pulse of the form of a hyperbolic secant² function. The contrast ratio is close to 3.0, in agreement with theoretical predictions.⁶

In order to ensure that the measured pulse duration was not limited by the spatial resolution of the imaging lens (L2, Fig. 3), the effective aperture (A) was varied without any significant effect on the width of the fluorescence profile. This indicates that the measured deviation of the pulses is greater than the resolution of the present optical system, which is estimated to be <100 fsec.

Conclusion

A relatively simple, reliable method of measuring the durations of individual subpicosecond UV laser pulses has been demonstrated. The technique should be applicable to ArF* and KrCl* as well as KrF* lasers with a resolution of <100 fsec.

The authors acknowledge fruitful discussions with T. S. Luk, U. Johann, A. P. Schwarzenbach, and K. Boyer. The technical assistance of R. Slagle, J. Wright, T. Pack, and R. Bernico is also acknowledged. This research was supported by the U.S. Office of Naval Research, the U.S. Air Force Office of Scientific Research, the Strategic Defense Initiative Organization (Innovative Science and Technology Office), the U.S. Department of Energy, the Lawrence Livermore National Laboratory, the National Science Foundation, the Defense Advanced Research Projects Agency, and the Los Alamos National Laboratory.

* Permanent address, The Blackett Laboratory, Imperial College, London SW7 2BZ, UK.

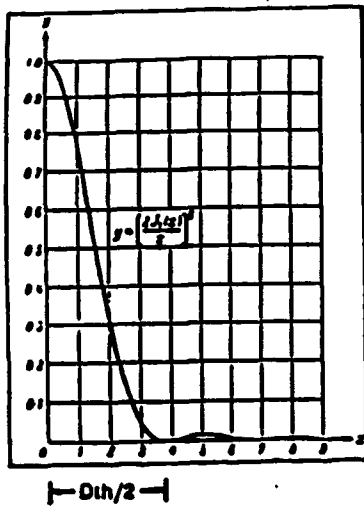
References

1. A. L'Huillier, L.-A. Lompré, G. Mainfray, and C. Manus, *Phys. Rev. Lett.* **48**, 1814 (1982); *Phys. Rev. A* **27**, 2503 (1983).
2. U. Johann, T. S. Luk, I. A. McIntyre, A. McPherson, A. P. Schwarzenbach, K. Boyer, and C. K. Rhodes, "Multiphoton ionization in intense ultraviolet laser fields," in *Proceedings of the Topical Meeting on Short Wavelength Coherent Radiation* (American Institute of Physics, New York, to be published).
3. C. K. Rhodes, *Science* **229**, 1345 (1985).
4. J. H. Glowina, G. Arjavalingham, P. P. Sorokin, and J. E. Rothenburg, *Opt. Lett.* **11**, 79 (1986).
5. A. P. Schwarzenbach, T. S. Luk, I. A. McIntyre, U. Johann, A. McPherson, K. Boyer and C. K. Rhodes, *Opt. Lett.* **11**, 499 (1986).
6. Detailed reviews of techniques for ultrashort pulse measurements are given by D. J. Bradley and G. H. C. New, *Proc. IEEE* **62**, 313 (1974) and E. P. Ippen and C. V. Shank, in *Ultrashort Light Pulses*, S. L. Shapiro, ed. (Springer-Verlag, Berlin, 1977), p. 83.
7. M. Rothschild, W. Gornik, J. Zavelovich, and C. K. Rhodes, *J. Chem. Phys.* **75**, 3794 (1981).
8. S. E. Harris, A. H. Kung, E. A. Stappaerts, and J. K. Young, *Appl. Phys. Lett.* **23**, 232 (1973).
9. J. S. Cohen and R. T. Pack, *J. Chem. Phys.* **61**, 2372 (1974).
10. O. Vallee, N. Traw Minh, and J. Chappelle, *J. Chem. Phys.* **73**, 2784 (1980).
11. R. S. Mulliken, *J. Chem. Phys.* **52**, 5170 (1970).
12. C. W. Werner, E. V. George, P. W. Hoff, and C. K. Rhodes, *IEEE J. Quantum Electron.* **QE-13**, 769 (1977).
13. A. W. Johnson and J. B. Gerardo, *J. Chem. Phys.* **59**, 1738 (1973).

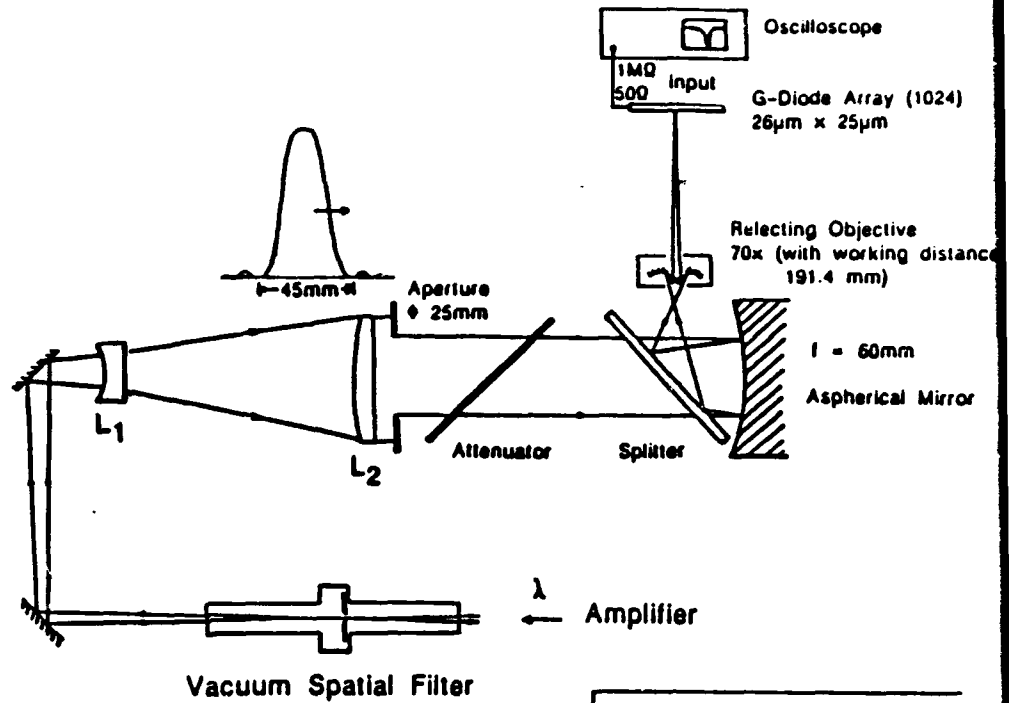
Appendix D: "Measurement of 248-nm Focal Volume Spatial Profiles"

MEASUREMENT OF 248-nm FOCAL VOLUME SPATIAL PROFILES

In order to confidently determine the experimental intensities involved in our measurements, it has been necessary to develop an accurate and reliable means for the measurement of spatial profiles of focal regions. Fig. (D-1) illustrates the apparatus that we have used for that purpose. The result of the measurement is shown in Fig. (D-2). The measured width of $\sim 1.43 \mu\text{m}$ is seen to agree with the corresponding ideal of $1.45 \mu\text{m}$. These results demonstrate that the beam is at the transform limit and that spot sizes on the order of $1 \mu\text{m}$ can be produced.



$$D_{th} = 2.44 \cdot \lambda \cdot f / d \text{ (}\mu\text{m)}$$



- L_1 : $f = -1\text{m}$, $\phi 25\text{mm}$
- L_2 : $f = 4\text{m}$, $\phi 34\text{mm}$
- $\lambda = .248 \mu\text{m}$
- $d = 25 \text{ mm}$
- $f = 60 \text{ mm}$

Focus Point Size Measurement

Fig. (D-1): Apparatus used to measure the spatial profiles of focal regions for subpicosecond 248-nm radiation.

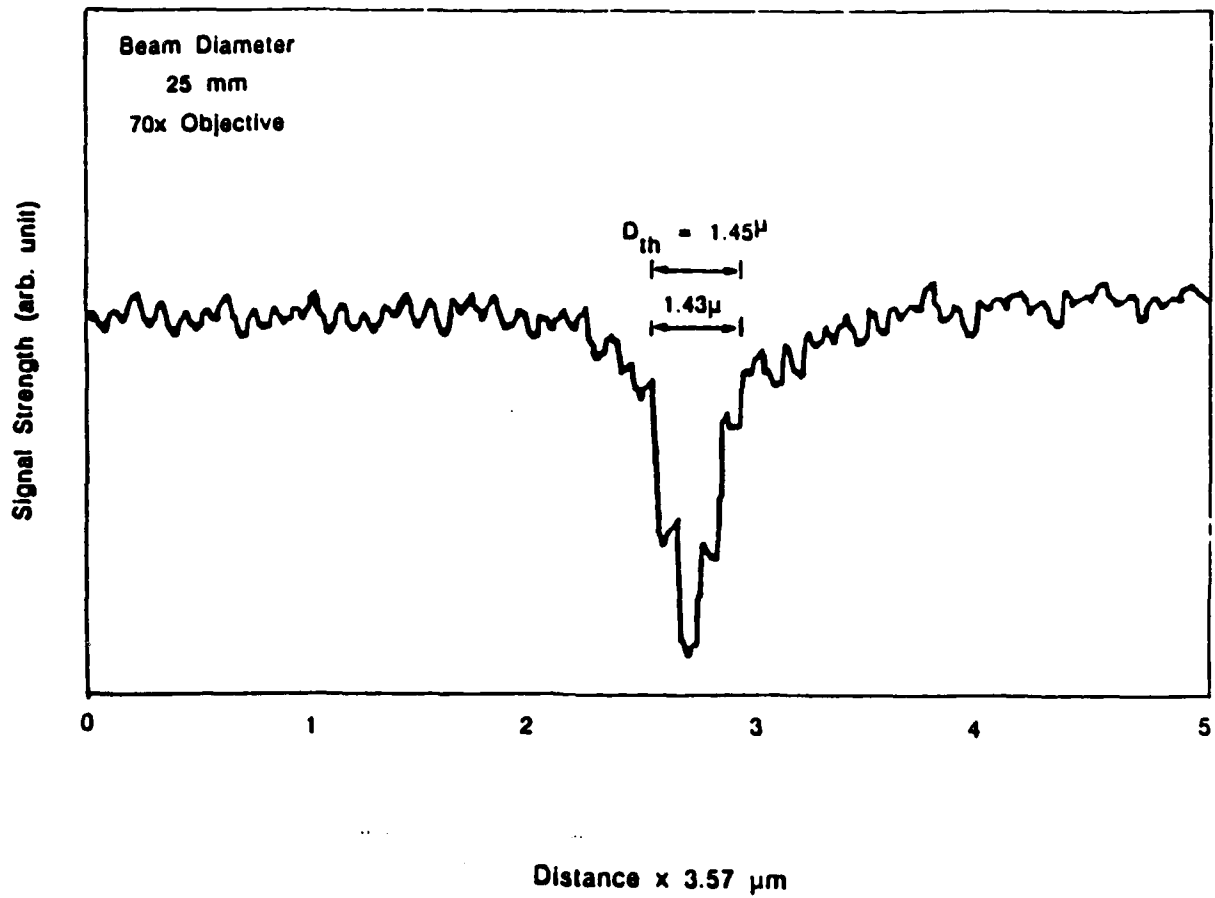


Fig. (D-2): Measured focal spot size with f/2 mirror. The measured width is ~ 1.43 μ m, a value to be compared with the corresponding theoretical ideal of 1.45 μ m.

Appendix E: "Characteristics of a Non-Equilibrium Picosecond Laser Plasma"

CHARACTERISTICS OF A NON-EQUILIBRIUM
PICOSECOND LASER PLASMA *

G. Gibson, R. Rosman, T. S. Luk, I. A. McIntyre
A. McPherson, G. Wendin,† K. Boyer and C. K. Rhodes
Laboratory for Atomic, Molecular, and Radiation Physics
Department of Physics, University of Illinois at Chicago
P. O. Box 4348, Chicago, Illinois 60680

Abstract

VUV spectra of a highly ionized argon plasma produced by a high-power subpicosecond laser are analyzed to determine the electron temperature. The calculated electron temperature is too low to support the highest observed charge state, showing the plasma charge state distribution to be out of Saha equilibrium.

Introduction

Unusual states of highly ionized plasmas can be generated over a wide range of electron densities with the use of high-power subpicosecond ultraviolet lasers. Plasmas created by such means should have characteristics quite different from those produced by traditional techniques involving current-pinch or laser radiation in the much longer nanosecond time regime. Generally, the conventional approaches involve electron collisions over a considerable time period (e.g. $\sim 10^{-9}$ sec) as the main mechanism producing the higher charge states. Consequently, this process often can be well described in thermodynamic terms. In contrast, plasmas produced by multi-photon ionization on a subpicosecond time scale involve a high level of ionization, low electron heating, negligible ion heating, and insignificant heavy-body hydrodynamic motion. This type of plasma is perfectly suited to recombination laser schemes: the low electron temperature leads to rapid recombination, the low ion temperature reduces doppler broadening, and, most importantly, the initial charge state distribution can be substantially out of thermal equilibrium.

This work presents VUV spectra of argon plasmas produced by a high power subpicosecond ultraviolet laser over a wide range of laser power (10-300 GW) and electron density (2×10^{19} - 2×10^{20} cm⁻³). Most of the observed spectral

lines can be identified from Ar⁵⁺, Ar⁶⁺, and Ar⁷⁺ as well as a doublet from Ar³⁺. From the Ar⁷⁺ spectrum an electron temperature can be deduced by comparing the line intensities to calculated values. A value of 20 eV is obtained and found to be inconsistent with the observed Ar⁵⁺ radiation.

Experiment

As the laser, target, and spectrometer used in this experiment have been described in detail elsewhere [1,2,3,4], only a brief summary is presented here. Subpicosecond pulses at 745 nm are extracted from a hybridly mode-locked dye laser. These pulses are frequency tripled to 248 nm, pre-amplified by a commercial KrF⁺ excimer and spatially filtered. The pulses are then amplified by 1) a second commercial excimer to 10-20 mJ and focused with an F/14 spherical lens to a peak intensity $\sim 10^{16}$ Wcm⁻² or 2) the Prometheus amplifier system [4] to ~ 300 mJ and focused with an F/15 spherical lens to an estimated peak intensity of $\sim 5 \times 10^{16}$ Wcm⁻². The rather small increase in peak intensity for the more powerful beam is due to severe spherical aberration in the F/15 focusing lens. The target is produced by a pulsed valve giving densities of 2×10^{18} - 2×10^{19} cm⁻³. The radiation is observed by a McPherson grazing incidence spectrometer recording from 25-750 angstroms. The spectrometer was calibrated with a HeNe discharge lamp and fluorescence lines to an absolute accuracy of ± 0.3 angstroms.

Results

Fig. 1 shows a typical region of the spectrum produced by the 10 GW beam with identified transitions from various charge states as well as some possible new identifications. Almost all the lines were identified from published results for the Ar¹⁺, Ar²⁺, Ar³⁺, Ar⁴⁺, and Ar⁷⁺ spectra [5,6,7,8].

* to be published in the OSA Proceedings on Short Wavelength Coherent Radiation: Generation and Application, 26-29 September 1988, Cape Cod, Massachusetts, edited by R. W. Falcone and J. Kirz

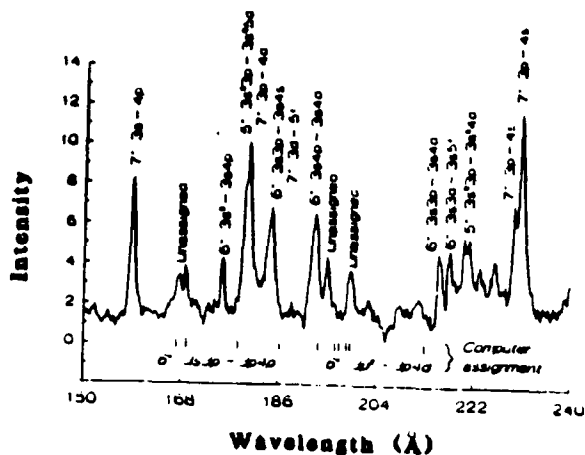


Fig. 1. Typical region of the argon spectrum taken with the 10 GW beam showing the assignments from the literature (above the spectrum) and the computer calculations (below the spectrum).

There was no evidence for radiation from the Ar^{2+} , Ar^{3+} , and Ar^{4+} charge states although these species have numerous transitions in the spectral range studied. Figure 2 shows a grotrian diagram of Ar^{7+} with the solid lines indicating the transitions observed in the plasma. The $n=3$ to $n=3$ transitions were not detected, possibly because of radiation trapping.

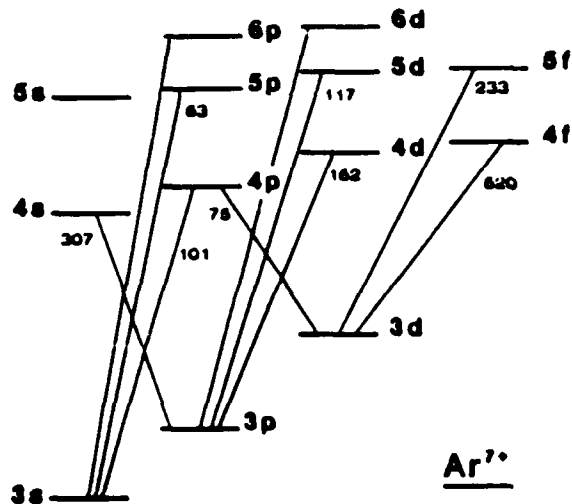


Fig. 2. Ar^{7+} grotrian diagram showing the observed transitions in the data. Transition rates (10^6 sec^{-1}) from Ref. 13 are shown for each line.

In an attempt to identify the remaining features in the spectrum, doubly excited transitions in Ar^{8+} were calculated with the computer code developed by Cowan [9], as transitions of this type are not commonly reported in the literature. Four Ar^{8+} transitions were calculated: $3p^2-3p4s$, $3s3p-3p4p$, $3p^2-3p4d$, $3p3d-3p4f$. In all four cases, lines previously unidentified on the basis of

literature citation were seen in the spectrum at the calculated wavelengths. With literature values and the computer analysis, it was possible to assign over 85% of the argon lines in the range 100–300 Å.

The spectrum produced with the 300 GW beam was virtually identical to the 10 GW beam except for a prominent doublet shown in Fig. 3. This doublet can clearly be identified [6,8] as the $2s^22p^6-2s2p^6$ doublet in Ar^{8+} by the absolute measurement of the wavelength ($\pm 0.3 \text{ Å}$), the splitting of the doublet ($\pm 0.1 \text{ Å}$), and the consistency with the previous assignments. We considered the possibility that these were satellite lines, but ruled that out based on calculations [9] of satellite structures in both Ar^{7+} and Ar^{8+} .

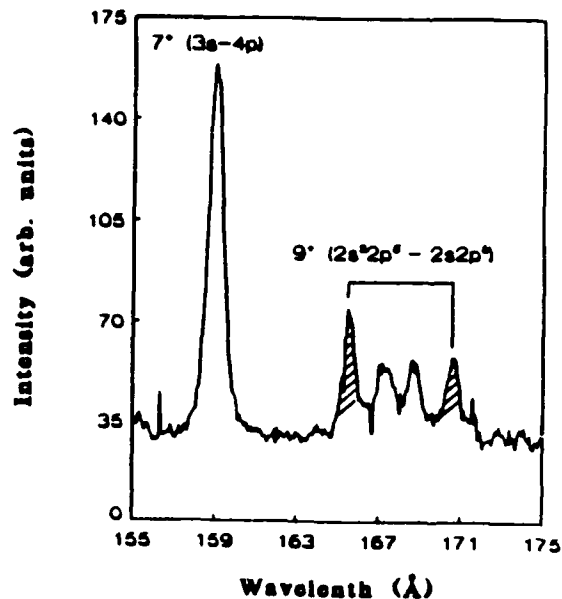


Fig. 3. Argon spectrum showing Ar^{8+} lines produced by the 300 GW beam.

In addition, detailed dependencies on the gas density of the target for the $Ar^{7+}(3s-4p)$ (159 Å) and the $Ar^{8+}(2s^22p^6-2s2p^6)$ (165 Å) transitions were obtained.

Discussion

To understand more about the argon plasma from the spectra, a plasma model was developed in order to calculate the effects of different electron temperatures and densities on the dynamics of the Ar^{6+} , Ar^{7+} , and Ar^{8+} ions. The model will be discussed in more detail elsewhere [10], but it is essentially a complete set of collisional-radiative rate equations in the spirit of Bates, Kingston and McWhirter [11]. Ar^{8+} is described simply as a ground state because of the large excitation energy of the lowest excited state (250 eV), all Ar^{7+} levels are included up to $n=7$, and the Ar^{7+} ground state is allowed to recombine to Ar^{8+} , although the details of the Ar^{8+} energy level structure were not explicitly included. Dielectronic recombination

from Ar^{8+} to Ar^{7+} was neglected [12] because of the closed shell structure of Ar^{8+} . Rate coefficients were obtained from a variety of sources [9,13,14].

The plasma electron temperature was calculated by comparing ratios of experimental line intensities for isolated transitions in the Ar^{7+} spectrum with numerical predictions of the plasma model. The results are shown in Fig. 4. Since the model had no free parameters, except the electron temperature and initial charge state distribution, the agreement between the data and the model for a temperature of 20 eV is remarkable. The discrepancy for the $Ar^{7+}(3d-4f)$ transition could be explained by its wavelength as it is rather different from the other transitions and so could be susceptible to systematic errors in the spectrometer. It is also possible that other processes are playing a role in determining the emission from this level. Further study of this matter is required. This value of 20 eV compares well with an electron spectrum taken with the 10 GW laser beam under collision free conditions at a somewhat lower intensity [15]. The data are shown in Fig. 5 and suggest an average electron kinetic energy of about 20 eV for the highest charge states. This would imply that no additional electron heating occurs in the gas target at the densities used in the present experiment.

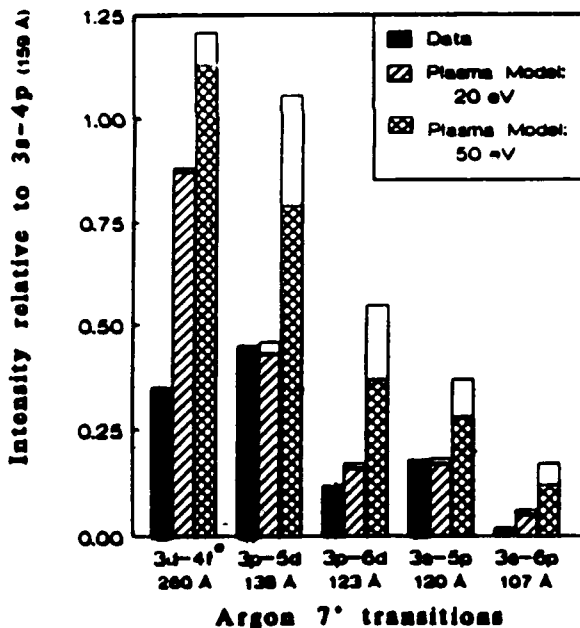


Fig. 4. Line intensities for selected Ar^{7+} lines normalized to the $Ar^{7+}(3s-4p)$ transition. Open regions in the bar correspond to varying the initial conditions in the plasma model. *All 3d-4f intensities are divided by 10.

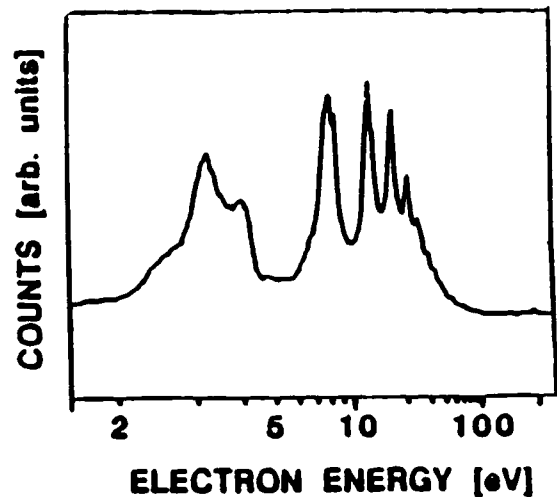


Fig. 5. Electron energy spectrum for argon at $7 \times 10^{16} \text{ Wcm}^{-2}$, from Ref. 15.

In addition to determining the electron temperature, the plasma model can predict the density dependence of the Ar^{7+} transitions. The results of the calculations and the experimental data from the 300 GW beam are compared in Fig. 6. Besides an overall scaling factor, the model had no free parameters except the electron temperature determined previously. However, one additional effect needed to be considered in order for the model to match the observed pressure dependence [10]. The spectral data are time integrated and, hence, the line intensities

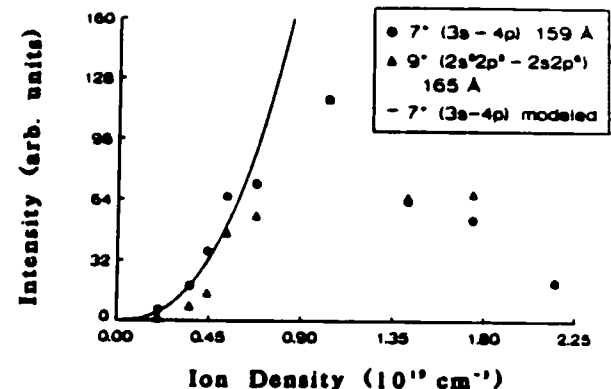


Fig. 6. Pressure dependencies of various lines, both experimental (300 GW beam) and modeled ($T_e = 20 \text{ eV}$). Turn over at higher densities is due to non-resonant absorption of the fluorescence by the surrounding gas.

depend on the lifetime of the plasma. The lifetime of the plasma, in turn, depends on the cooling rate of the plasma. Under these conditions, electron conduction cooling is the dominant cooling mechanism. As the thermal conductivity is inversely proportional to gas density, the lifetime of the plasma will be directly proportional to the gas density. Taking this effect into account, the plasma model correctly predicts the density dependence of the $\text{Ar}^{7+}(3s-4p)$ transition. Thus, the line radiation from Ar^{7+} is consistent with a collisional-radiative model with an electron temperature of ~ 20 eV.

The Ar^{8+} line in Fig. 6 is similar to the Ar^{7+} line in that it is a ground state transition and has about the same excitation energy [6,8] and transition probability [9]. Thus, it is not surprising that it has a similar density dependence. However, the origin of the Ar^{8+} ions is not so clear. Although they could have been produced by multi-photon ionization, preliminary ion measurements with the same laser system and focusing lens did not detect any Ar^{8+} ions [16]. On the other hand, an electron density of $5 \times 10^{19} \text{ cm}^{-3}$ and temperature of 20 eV cannot support Ar^{8+} in Saha equilibrium [14]. The ratio of Ar^{8+} to Ar^{7+} ions under these conditions would be less than 10^{-5} . Thus, 20 eV is not a high enough temperature to substantially ionize Ar^{8+} . The Ar^{8+} radiation could have been produced earlier in time at a higher temperature. However, Ar^{8+} radiation would have been produced at the same time, and none was observed. Alternatively, the Ar^{8+} ions may be in a different region of space, perhaps at a higher temperature. The region of Ar^{8+} is most likely surrounded by Ar^{7+} and calculations of electron conduction cooling [10] show that spatial variations in temperature rapidly decay. The electrons in the Ar^{8+} region would quickly equilibrate with the surrounding electrons.

The most consistent explanation is that the laser pulse creates a plasma, through a process not yet understood, containing Ar^{7+} , Ar^{8+} , and Ar^{9+} with an initial electron temperature of 20 eV. This temperature can excite the Ar^{7+} states, the first excited state of Ar^{8+} , but nothing in Ar^{9+} . This situation is consistent with all the experimental and calculated results presented in this paper and shows that it is possible to create a higher charge state than can be supported in Saha equilibrium.

Conclusion

VUV spectra of a highly ionized argon plasma produced by a high power subpicosecond laser are presented along with calculations from a plasma model. Comparison of the two show that the observed Ar^{7+} radiation is fully consistent with a collisional-radiative model of the plasma with an electron temperature of 20 eV. Furthermore, comparing this electron temperature with a collision-free electron energy spectrum shows that little additional heating of the electrons occurred in the dense gas target. Finally, observation of Ar^{8+}

radiation indicates that the charge state distribution is not in Saha equilibrium as the electron temperature and density of the plasma can not support the Ar^{8+} charge state.

Acknowledgements

The authors would like to thank J. Peek for providing the Cowan code and indispensable help in implementing it, and P. Noel, R. Slagle, and J. Wright for their technical assistance. This work was supported by AFOSR, LLNL, ONR, NSF, and SDI.

† permanent address: Institute of Theoretical Physics, Chalmers Institute of Technology, Fysikgränd 3, S-412 90 Göteborg, Sweden

References

1. A. McPherson, G. Gibson, H. Jara, U. Johann, T. S. Luk, I. A. McIntyre, K. Boyer and C. K. Rhodes, "Studies of Multiphoton Production of Vacuum Ultraviolet Radiation in the Rare Gases," *J. Opt. Soc. Am.* **B4**, 595 (1987).
2. C. K. Rhodes, "Physical Processes at High Field Strengths," *Physica Scripta*, **T17**, 193 (1987).
3. A. P. Schwarzenbach, T. S. Luk, I. A. McIntyre, U. Johann, A. McPherson, K. Boyer and C. K. Rhodes, "Subpicosecond KrF^* Excimer-Laser Source," *Optics Letters* **11**, 499 (1986).
4. I. A. McIntyre, T. S. Luk, G. Gibson, H. Jara, A. McPherson, X. J. Pan, K. Boyer and C. K. Rhodes, "Ultrahigh Intensity KrF^* Laser," to be submitted to *Optics Letters*.
5. I. Iesteven-Vaisse, M. Chantepie, J. P. Grandin, D. Hennecart, X. Husson, D. Lecler, J. P. Buchet, M. C. Buchet-Poullizac, J. Desesquelles, and S. Martin, "VUV Spectra of Multicharged Recoil-Ions: Neon and Argon," *Physica Scripta* **34**, 138 (1986).
6. R. L. Kelly and L. J. Palumbo, "Atomic and Ionic Emission Lines Below 2000 Å," N.R.L. Report 7599 (1973).
7. B. C. Fawcett, A. Ridgeley and G. E. Bromage, "The Spectrum ArIX and Extended Spectral Classification in ArV to ArVIII and ArX ," *Physica Scripta* **18**, 315 (1978).
8. R. Engleman, Jr., D. B. Thomson and D. A. Monaghan, "Vacuum Ultraviolet Emission from Argon, Krypton, and Xenon in a Radial-Viewed Theta Pinch," LANL Report LA-6275-MS (1976).
9. R. D. Cowan, *The Theory of Atomic Structure*

- and Spectra (University of California Press, Berkeley, 1981) and J. Peek, private communication.
10. G. Gibson, et al., "Recombination Lasers Using Multiphoton Ionization," to be submitted.
 11. D. R. Bates, A. E. Kingston, and R. W. P. McWhirter, "Recombination between Electrons and Atomic Ions," Proc. Roy. Soc. A267, 297 (1962).
 12. J. M. Shull and M. van Steenberg, "The Ionization Equilibrium of Astrophysically Abundant Elements," Astrophys. J. Suppl. Ser. 48, 95 (1982).
 13. R. U. Dalta, H.-J. Kunze, and D. Petrini, "Collisional-Rate Coefficients for Sodiumlike ArVIII Ions," Phys. Rev. A8, 38 (1972).
 14. H. R. Griem, Plasma Spectroscopy (McGraw-Hill, New York, 1964).
 15. U. Johann, T. S. Luk, I. A. McIntyre, A. McPherson, A. P. Schwarzenbach, K. Boyer and C. K. Rhodes, "Multiphoton Ionization in Intense Ultraviolet Laser Fields," in Proceedings of the Topical Meeting on Short Wavelength Coherent Generation, ed. D. T. Attwood and J. Bokor, AIP Conference Proceedings No. 147 (AIP, New York, 1986) p. 202.
 16. T. S. Luk, private communication.

Appendix F: "X-Ray Amplification with Charge-Displacement Self-Channeling"

**X-RAY AMPLIFICATION WITH
CHARGE-DISPLACEMENT SELF-CHANNELING***

J. C. Solem,[†] T. S. Luk, K. Boyer, and C. K. Rhodes
Laboratory for Atomic, Molecular, and Radiation Physics
Department of Physics, University of Illinois at Chicago
P. O. Box 4348, Chicago, Illinois 60680

ABSTRACT

We develop an analytic theory of charge-displacement self-channeling: a mechanism that can dynamically trap a short intense light pulse in the refractive index gradient created by the ponderomotive expulsion of free electrons. The channel is an effective waveguide for secondary radiation and its radius increases very slowly with power. We expect large energy deposition rates from multiphoton coupling, making the channel ideal for generating coherent short wavelength radiation.

* Resubmitted to Phys. Rev. Lett., 29 September 1988

† permanent address, Theoretical Division, MS-B210, Los Alamos National Laboratory, Los Alamos, New Mexico 87545

Amplification in the x-ray region requires prodigious energy deposition rates¹ spatially organized in a high-aspect-ratio volume of material. We show that the use of extremely intense ($10^{19} - 10^{22}$ W/cm²) short pulse (~ 100 fs) radiation may be able to produce these conditions by combining (1) the energy deposition^{2,3} arising from high-order multiphoton processes with (2) a new mode of channeled propagation involving a charge-displacement mechanism. It is significant that the conditions needed for the strong multiphoton coupling are identical to those found required for the confined propagation. Since previous work² discusses the energy deposition rates, the present discussion concentrates on the propagation.

The presence of a very intense pulse of radiation in a highly ionized plasma produced by multiphoton ionization leads to the following qualitative behavior. The conversion of electrons from bound to free states by the ionization induces a strong reduction in the refractive response of the atomic material. The resulting plasma exhibits a further decrease in index from the free electron component produced. Assuming that the frequency ω of the radiation is above the plasma frequency ω_p , these circumstances permit a new mode of channeled propagation to develop. For a sufficiently short pulse (~ 100 fs), the ions remain spatially fixed while the relatively mobile electrons are expelled by the ponderomotive potential from the high intensity region of the beam. A state of equilibrium can then be established between the ponderomotive and the electrostatic force densities owing to the net charge displacement. Since the electrons, which embody a negative contribution to the index, are expelled, an on-axis region of relatively high refractive index is formed which can support the channeling. Some aspects of this behavior have been recently examined in the regime of low plasma density.⁴

The state of ionization and its radial profile are important aspects of the analysis. For these estimates, we use the formulation of Keldysh⁵ corresponding

to the situation in which tunneling dominates,^{6,7} and have included a correction for the effect of the Coulomb field in the final state.⁷ The influence of atomic shell structure is accounted for through the use of computed ionization potentials for multiply charged ions.⁸ An example involving holmium illustrates the outcome of this procedure. It is found that for a pulse of 100 fs duration, nickel like holmium (Ho^{31+}) will be produced for intensities spanning the $1.3 - 4.8 \times 10^{20}$ W/cm² range. Therefore, if the spatial beam profile were a gaussian having a radial dimension r_0 and a peak intensity $I_0 = 4.8 \times 10^{20}$ W/cm², the nickel state would exist from $r = 0$ to $r = 1.3r_0$, nearly the entire region of interest.

The radial dependence of the refractive index $n(r)$ governs the condition for channeling. Since the ions are inertially confined for the short time (~ 100 fs) considered, the expulsion of the free electrons from the channel results in a reduced plasma frequency or, equivalently, an increase of the refractive index in the central region.

The contribution to the index from the ions under the strong-field condition involves two opposing effects. They are (1) the nonlinear contribution proportional to n_2 , which is enhanced at more elevated field strengths, and (2) the tendency to produce high charge states, corresponding to low polarizabilities and depressed values of n_2 . The resulting ionic component of the index, however, is overwhelmed by the free electron contribution. This fact is demonstrated by another example involving Ho at an intensity of 3.7×10^{19} W/cm², the value at which Ho becomes krypton-like (Ho^{31+}). The index, through the first nonlinear term, is $n = 1 + n_0 + n_2 E^2$, with $n_0 = 2\pi n_a \alpha_0$ and $n_2 = (\pi/3)n_a \alpha_2$. We can relate these susceptibilities for Ho^{31+} to known values⁹ for neutral Kr, namely, $\alpha_0 = 24.8 \times 10^{-28}$ esu and $\alpha_2 = 137.7 \times 10^{-28}$ esu. Since Ho^{31+} has a radius of ~ 0.032 that of Kr, hydrogenic scaling yields $\alpha_0 = 10^{-28}$ esu and $\alpha_2 = 10^{-48}$ esu for Ho^{31+} . At the given intensity,

the ionic contribution then is $(n-1)_{at} \approx 10^{-28} n_a$, with n_a representing the ion density.

For a collisionless (Ho^{31+}) plasma with an electron density of $31n_a$, we obtain the free electron contribution to the index at 248 nm as $(n-1)_e \approx -(\omega_p^2/2\omega^2) = -8.5 \times 10^{-22} n_a$ so that $(n-1)_e/(n-1)_{at} \approx -10^7$. The free electron component is far larger than the ionic contribution and can be safely neglected.

The steady-state force balance between the radially outward ponderomotive force and the oppositely directed electron-ion attraction is represented in cylindrical symmetry for a completely ionized tenuous ($\omega \gg \omega_p$) plasma by

$$\frac{2\pi e^2}{m\omega^2 c} \nabla I(r) + e^2 n_e \int \frac{\rho(r') (r - r')}{|r - r'|^3} d^3 r' = 0 \quad (1)$$

For a gaussian intensity distribution $I(r)$ the charge density $\rho(r)$ is

$$\rho(r) = 2B [1 - (r/r_0)^2] e^{-(r/r_0)^2} \quad (2)$$

in which $B = I_0(m\omega^2 c n_e r_0^2)^{-1}$ and m , c , n_e , and r_0 denote the electron mass, speed of light, quiescent plasma density, and channel radius, respectively.

An estimate of the condition necessary for focusing can now be made by describing the charge displacement by two regions such that $\rho(r < r_0\sqrt{2}) = \rho(0)$ and $\rho(r > r_0\sqrt{2}) = \rho(r_0\sqrt{2})$ and equating the angle of total internal reflection to the angle corresponding to the first minimum of diffraction. This yields a critical intensity

$$I_C = \frac{\pi m \omega^2 c}{64(1 + e^{-2}) r_e} \approx (4.3 \times 10^{-3}) \frac{m \omega^2 c}{r_e} \quad (3)$$

in which r_e denotes the classical electron radius. Significantly, this intensity is independent of the electron density n_e and contrasts with the power threshold¹⁰ normally arising from induced index changes in transparent dielectrics. Analytic approximations extending to high electron density show a significant dependence of I_C on n_e only near the critical density. Furthermore, it is easily demonstrated that I_C normalized to the Compton intensity is a constant (0.54) independent of

frequency, a finding which shows that the charge-displacement mechanism is associated with relativistic conditions.

If the intensity exceeds I_C , the beam will tend to form a channel and, if $B < 1/2$, Eq. (2) properly describes the charge density. However, since the range $B < 1/2$ is quite narrow, the situation involving $B > 1/2$, the "saturated" condition in which all free electrons are expelled from the core of the channel, is of principal interest. An estimate of the radius r_s of the saturated region [$\rho(r < r_s) = 1$] can be made by modeling the channel as a dielectric waveguide. It is assumed that the expelled electrons form a cylindrical sheath around the saturated region with a thickness comparable to r_s so that $\rho(r_s < r < 2r_s) = -1/3$ and $\rho(r > 2r_s) = 0$. Consequently, the charge density ρ changes from 1 to $-1/3$ at the interface. The cutoff frequency ω_C of the dielectric waveguide¹¹ can be written as

$$\omega_C = \frac{x_{01}c}{r_s(\omega_p/\omega)[\rho(r < r_s) - \rho(r > r_s)]^{1/2}} \quad (4)$$

in which x_{01} is the first root of $J_0(x)$. Setting $\omega \lesssim \omega_C$, we find $r_s \approx (x_{01}c)(3/4)^{1/2}\omega_p^{-1} \approx 2c/\omega_p$ giving the power P_s for the onset of saturation ($B = 1/2$) as

$$P_s \approx \frac{2mc^3}{r_e} \left(\frac{\omega}{\omega_p}\right)^2 = (1.74 \times 10^{10}) \left(\frac{\omega}{\omega_p}\right)^2 \text{ W.} \quad (5)$$

Examination of the strongly saturated case in the limit of high intensity ($I_0 \gg 2.3 \times 10^{21} \text{ W/cm}^2$), shows that complete expulsion of the electrons extends out to a radius

$$r_s \approx \frac{c}{\omega_p} (2\beta I_0^{1/2} - 2)^{1/2}, \quad (6)$$

where

$$\beta = \left(\frac{J_1(x_{01})x_{01}}{\omega}\right) \left(\frac{4\pi r_e}{mc}\right)^{1/2}. \quad (7)$$

Thus, the dependence of r_s on intensity is extremely weak. Furthermore, the

intensity distribution is well approximated by

$$I(r) = \begin{cases} I_0 J_0^2(qr) & ; r \leq r_s \\ \frac{m\omega^2 c}{4\pi r_e} \exp[2(r_s - r)/\delta] & ; r > r_s \end{cases} \quad (8)$$

in which $\delta = (2\pi n_e r_e r_s)^{-1}$ and $q = \alpha_0 (\delta + r_s)^{-1}$.

The validity of the motionless-ion approximation is readily established. The ponderomotive force on an ion is proportional to its charge ζ and inversely proportional to its mass M . For Ho at $I_0 \sim 4.8 \times 10^{20}$ W/cm², the ponderomotive force moves an ion a distance $\sim 4 \times 10^{-10}$ that of an electron, a negligible distance.

A far larger force on the ions results from the charge displacement itself, since their mutual electrostatic repulsion will expel them from the beam. However, the ion motion due to this force is also small for a sufficiently short pulse. Assume that the saturated channel has been formed at $t = 0$. With the electrostatic force on an ion at radius $r < r_s$, given as $F = 2\pi r (\zeta e)^2 n_a$ by Gauss' law, an ion with initial position r_0 has its motion described by $r = r_0 \exp(y^2)$ where

$$\int_0^y \exp(y'^2) dy' = [\pi \zeta^2 r_e c^2 n_a (m/M)]^{1/2} t, \quad (9)$$

a statement which leads to the approximate result for small displacements of

$$\frac{r - r_0}{r_0} \approx \pi \zeta^2 r_e c^2 n_a (m/M) t^2. \quad (10)$$

At $I_0 = 4.8 \times 10^{20}$ W/cm², the ion migration gives a relative change in the radius of about 9% after 100 fs.

The two principal mechanisms leading to energy loss in the channel are (1) ionization and (2) the field energy associated with the charge displacement. The energy lost to ionization can be found by summing the ionization potentials⁸ of electrons successively stripped from the atom up to the ionization level produced by the field. For the Ho³⁹⁺ case, with $n_a = 2.3 \times 10^{18}$ cm⁻³ and a channel

radius $r_s \approx 2c/\omega_p = 1.1 \mu\text{m}$, ionization produces a loss of $\sim 4.3 \text{ mJ/cm}$ while charge displacement accounts for $\sim 160 \text{ mJ/cm}$.

In the strongly saturated case, the charge density $\rho(r)$ has the form

$$\rho(r) = \begin{cases} 1 & , r < r_s \\ r_s/\delta & , r_s < r < r_s + \delta \\ 0 & , r \geq r_s + \delta \end{cases} \quad (11)$$

from which the radially directed field $E(r)$ can be computed according to

$$E(r) = \frac{4\pi en_e}{r} \int_0^r \rho(r') r' dr' \quad (12)$$

By direct integration, the charge-displacement field energy per unit length of the channel $d\epsilon_c/dx$, in the limit $I_0 \gg 2.3 \times 10^{21} \text{ W/cm}^2$, is given by

$$\frac{d\epsilon_c}{dx} = \frac{\pi^2 e^2 r_e}{2} n_e^2 \left(\frac{c}{\omega_p} \right)^6 (2\beta I_0^{1/2} - 2)^2 \quad (13)$$

Two questions concerning the stability of such channels have been examined. The first involves energetic stability associated with the splitting of a single channel into two or more having a reduced total electrostatic energy. The second considers stability against relativistic self-focusing in the walls of the channel, a mode observed in recent numerical simulations.¹²

For appraisal of the case based on energetics, using the approximation

$$\int_0^x J_0^2(x') x' dx' \approx 1/2 x_0^2 J_1^2(x_0) [1 - (1 - x/x_0)^{2.2}]^2 \quad (14)$$

which is accurate to within ten percent over the $0 < x \leq x_0$ range, for a total power $P = P_0 + P_1$, we find that inside the saturated region

$$P_0 = 2\pi I_0 \int_0^{r_s} J_0^2(qr) r dr = \frac{J_1^2(x_0) \beta^2 I_0^2}{2n_e r_e (\beta I_0^{1/2} - 1)} [(1 - \beta I_0^{1/2})^{-2.2}]^2 \quad (15)$$

while in the region outside

$$P_1 \approx \frac{mc\omega^2}{2r_e} \int_{r_s}^{\infty} \exp(2(r_s - r)/\delta) r dr \approx \frac{mc\omega^2}{16\pi n_e r_e^2} \quad (16)$$

With Eqs. (6), (13), and (15) and taking the limit $\beta^2 I_0 \gg 1$, we find further

$$\frac{\epsilon_C}{\ell} \approx \frac{\beta^2 n_0 m c^2}{8 J_1^2(x_{01})} P \quad (17)$$

a result which shows that the electrostatic energy ϵ_C per unit length ℓ scales directly as the laser power. Therefore, this energy would not be reduced by splitting into two channels with half the power. Further inspection of Eqs. (6), (13), and (15) shows that an even more stable situation exists for powers less than the asymptotic limit.

The total power propagating in the channel walls is given by Eq. (16). The power threshold for relativistic self-focusing^{13,14} is $P_r = k m \omega^2 (4 \pi n_0 e^2)^{-1}$, in which $k = 1.5 \times 10^{10}$ W, so that the condition $P_r > P_1$, barring relativistic self-focusing in the walls is $k > m c^3 (4 r_0)^{-1}$, a provision satisfied by the result 2.2×10^7 W $< 1.5 \times 10^{10}$ W. Relativistic filamentation in the walls is suppressed for a strongly saturated channel.

Several additional considerations are pertinent. We see that if the frequency ω exceeds the cutoff in Eq. (4), a condition essential for the channel to form, then all higher frequencies will also be guided. This occurs because the index is dominated by the free electrons or, equivalently, the angle of total internal reflection is proportional to the angle of the first minimum of diffraction. Since all of the radiation which falls within the acceptance angle of the waveguide will propagate as a guided mode, these channels can serve naturally as bright directed sources of energetic radiation.

Energy deposition rates associated with such channels are expected to be extremely high. Extrapolation² of experimental energy-transfer rates suggests that the multiphoton absorption cross section will limit to a frequency independent value of $\sim 10^{-20}$ cm² for heavy elements at intensities above 10^{19} W/cm², a value

near the Compton intensity in the ultraviolet. For the holmium case cited above, with an electron density $n_e \sim 8.9 \times 10^{19} \text{ cm}^{-3}$, the rate is in excess of 10^{19} W/cm^2 , a value far above that needed for amplification of radiation in the kilovolt region.¹

The scaling of the deposition rate on the primary laser frequency ω is strong. When $r_s \approx 2c/\omega_p$, channels with the same values of ω/ω_p are analogous; they have the same density and intensity distributions with power scaled as ω^{-2} and linear dimensions scaled as ω^{-1} . Consequently, power requirements scale with ω^{-2} for a fixed deposition rate. When the channel is strongly saturated, Eq. (16) applies, and power requirements scale as ω^{-3} . Furthermore, higher frequencies generally allow shorter transform-limited pulse lengths, enabling the ions to remain motionless at an increased power. Summed up, since the ion migration varies approximately as the square of the pulse length, the overall scaling could vary as rapidly as ω^5 . Finally, the charge-displacement energy, given in Eq. (13), scales as ω^{-3} for the strongly saturated case while the corresponding ionization energy goes as ω^{-3} .

Nonlinear absorption and channeled propagation combine cooperatively in producing conditions favorable to the use of intense short pulse ultraviolet radiation for the production of x-ray amplification. The ability to channel both the energy deposition and resulting emission can enormously increase the short wavelength gain and provide a natural mechanism for generating low-divergence high brightness x-ray sources.

Valuable discussions with George N. Gibson and Xiao-Jiang Pan are acknowledged. This work was supported by the AFOSR, the LLNL, the NSF, the ONR, and the SDIO.

References

1. A. V. Vinogradov and I. I. Sobel'man, *Sov. Phys.-JETP* **36**, 1115 (1973).
2. K. Boyer, H. Jara, T. S. Luk, I. A. McIntyre, A. McPherson, R. Rosman, and

- C. K. Rhodes, *Revue Phys. Appl.* **22**, 1793 (1987).
3. J. Cobble, G. Kyrala, A. Hauer, A. Taylor, C. Gomez, N. Delameter, and G. Schappert, "Kilovolt X-Ray Spectroscopy of a Subpicosecond Laser Excited Source," LAUR-88-1181, submitted to *Phys. Rev. Lett.*
 4. G.-Z. Sun, E. Ott, Y. C. Lee, and P. Guzdar, *Phys. Fluids* **20**, 526 (1987).
 5. L. V. Keldysh, *Sov. Phys.-JETP* **20**, 1307 (1965).
 6. S. Stenholm, *Contemp. Phys.* **20**, 37 (1979); P. Lambropoulos, *Advances in Atomic and Molecular Physics*, Volume 12, D. R. Bates and B. Pederson, eds. (Academic, NY, 1976) p. 86; H. B. Delone, *Sov. Phys.-Usp.* **18**, 169 (1975); T. P. Hughes, *Plasma and Laser Light* (Adam-Hilger, London, 1975), p. 145; C. Grey Morgan, *Rep. Prog. Phys.* **38**, 62 (1975).
 7. K. G. H. Baldwin and B. W. Boreham, *J. Appl. Phys.* **52**, 2627 (1981).
 8. T. A. Carlson, C. W. Nestor, Jr., N. Wasserman, and J. D. McDowell, *Atomic Data* **2**, 63 (1970).
 9. M. P. Bogaard and B. J. Orr, "Electric Dipole Polarizabilities of Atoms and Molecules," *Int. Rev. Sci.: Phys. Chem. Ser. 2*, ed. A. D. Buckingham, Vol. 2 (Butterworth, London, 1975) p. 149.
 10. P. L. Kelley, *Phys. Rev. Lett.* **15**, 1005 (1965).
 11. J. D. Jackson, *Classical Electrodynamics* (Wiley, New York, 1962) p. 259.
 12. W. B. Mori, C. Joshi, J. M. Dawson, D. W. Forslund, and J. M. Kindel, *Phys. Rev. Lett.* **60**, 1298 (1988).
 13. H. Hora, *Phys. Fluids* **12**, 182 (1969). Also see H. Hora, *Physics of Laser Driven Plasmas* (Wiley, NY, 1981) p. 72 - 153.
 14. C. E. Max, J. Arons, and A. B. Langdon, *Phys. Rev. Lett.* **33**, 209 (1974); P. Sprangle, C. M. Tang, and E. Esarey, *IEEE Trans. Plasma Sci.* **15**, 2 (1987).